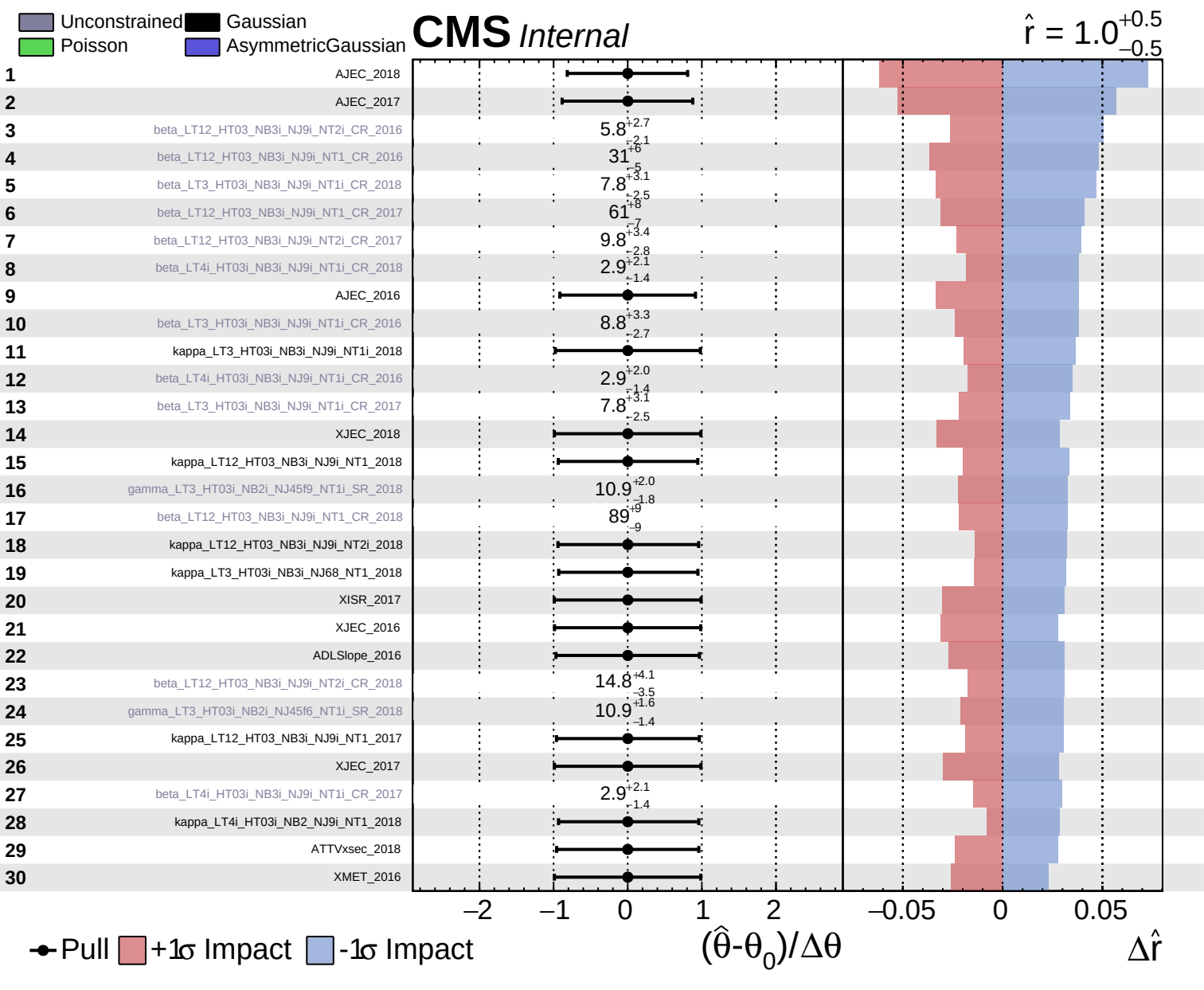
Unconstrained
Gaussian
Poisson
AsymmetricGaussian
CMS Internal
$\hat{r} = 1.0^{+0.5}_{-0.5}$
1 AJEC_2018
2 AJEC_2017
3 beta_LT12_HT03_NB3i_NJ9i_NT2i_CR_2016
4 beta_LT12_HT03_NB3i_NJ9i_NT1_CR_2016
5 beta_LT3_HT03i_NB3i_NJ9i_NT1i_CR_2018
6 beta_LT12_HT03_NB3i_NJ9i_NT1_CR_2017
7 beta_LT12_HT03_NB3i_NJ9i_NT2i_CR_2017
8 beta_LT4i_HT03i_NB3i_NJ9i_NT1i_CR_2018
9 AJEC_2016
10 beta_LT3_HT03i_NB3i_NJ9i_NT1i_CR_2016
11 kappa_LT3_HT03i_NB3i_NJ9i_NT1i_2018
12 beta_LT4i_HT03i_NB3i_NJ9i_NT1i_CR_2016
13 beta_LT3_HT03i_NB3i_NJ9i_NT1i_CR_2017
14 XJEC_2018
15 kappa_LT12_HT03_NB3i_NJ9i_NT1_2018
16 gamma_LT3_HT03i_NB2i_NJ45f9_NT1i_SR_2018
17 beta_LT12_HT03_NB3i_NJ9i_NT1_CR_2018
18 kappa_LT12_HT03_NB3i_NJ9i_NT2i_2018
19 kappa_LT3_HT03i_NB3i_NJ68_NT1_2018
20 XISR_2017
21 XJEC_2016
22 ADLSlope_2016
23 beta_LT12_HT03_NB3i_NJ9i_NT2i_CR_2018
24 gamma_LT3_HT03i_NB2i_NJ45f6_NT1i_SR_2018
25 kappa_LT12_HT03_NB3i_NJ9i_NT1_2017
26 XJEC_2017
27 beta_LT4i_HT03i_NB3i_NJ9i_NT1i_CR_2017
28 kappa_LT4i_HT03i_NB2_NJ9i_NT1_2018
29 ATTVxsec_2018
30 XMET_2016
$5.8^{+2.7}_{-2.1}$
31^{+6}_{-5}
$7.8^{+3.1}_{-2.5}$
61^{+8}_{-7}
$9.8^{+3.4}_{-2.8}$
$2.9^{+2.1}_{-1.4}$
$8.8^{+3.3}_{-2.7}$
$2.9^{+2.0}_{-1.4}$
$7.8^{+3.1}_{-2.5}$
$10.9^{+2.0}_{-1.8}$
89^{+9}_{-9}
$14.8^{+4.1}_{-3.5}$
$10.9^{+1.6}_{-1.4}$
$2.9^{+2.1}_{-1.4}$
−2
−1
0
1
2
−0.05
0
0.05
Pull
+1σ Impact
-1σ Impact
$(\hat{\theta}-\theta_0)/\Delta\theta$
$\Delta\hat{r}$

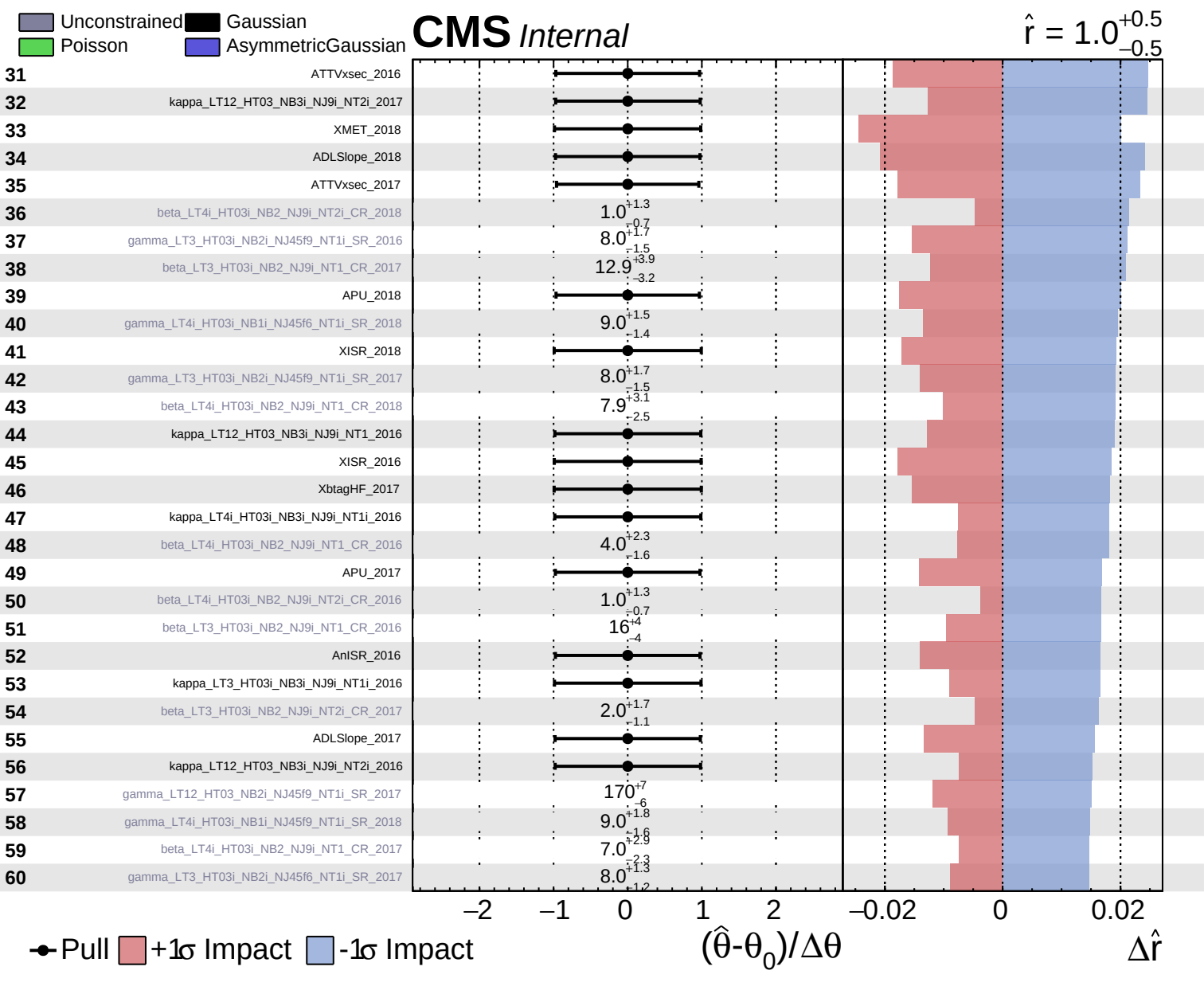
Unconstrained
Gaussian
Poisson
AsymmetricGaussian
CMS Internal
r̂ = 1.0 +0.5 −0.5
31 ATTVxsec_2016
32 kappa_LT12_HT03_NB3i_NJ9i_NT2i_2017
33 XMET_2018
34 ADLSlope_2018
35 ATTVxsec_2017
36 beta_LT4i_HT03i_NB2_NJ9i_NT2i_CR_2018 1.0 +1.3 −0.7
37 gamma_LT3_HT03i_NB2i_NJ45f9_NT1i_SR_2016 8.0 +1.7 −1.5
38 beta_LT3_HT03i_NB2_NJ9i_NT1_CR_2017 12.9 +3.9 −3.2
39 APU_2018
40 gamma_LT4i_HT03i_NB1i_NJ45f6_NT1i_SR_2018 9.0 +1.5 −1.4
41 XISR_2018
42 gamma_LT3_HT03i_NB2i_NJ45f9_NT1i_SR_2017 8.0 +1.7 −1.5
43 beta_LT4i_HT03i_NB2_NJ9i_NT1_CR_2018 7.9 +3.1 −2.5
44 kappa_LT12_HT03_NB3i_NJ9i_NT1_2016
45 XISR_2016
46 XbtagHF_2017
47 kappa_LT4i_HT03i_NB3i_NJ9i_NT1i_2016
48 beta_LT4i_HT03i_NB2_NJ9i_NT1_CR_2016 4.0 +2.3 −1.6
49 APU_2017
50 beta_LT4i_HT03i_NB2_NJ9i_NT2i_CR_2016 1.0 +1.3 −0.7
51 beta_LT3_HT03i_NB2_NJ9i_NT1_CR_2016 16 +4 −4
52 AnISR_2016
53 kappa_LT3_HT03i_NB3i_NJ9i_NT1i_2016
54 beta_LT3_HT03i_NB2_NJ9i_NT2i_CR_2017 2.0 +1.7 −1.1
55 ADLSlope_2017
56 kappa_LT12_HT03_NB3i_NJ9i_NT2i_2016
57 gamma_LT12_HT03_NB2i_NJ45f9_NT1i_SR_2017 170 +7 −6
58 gamma_LT4i_HT03i_NB1i_NJ45f9_NT1i_SR_2018 9.0 +1.8 −1.6
59 beta_LT4i_HT03i_NB2_NJ9i_NT1_CR_2017 7.0 +2.9 −2.3
60 gamma_LT3_HT03i_NB2i_NJ45f6_NT1i_SR_2017 8.0 +1.3 −1.2
−2 −1 0 1 2
−0.02 0 0.02
Pull +1σ Impact -1σ Impact
(θ̂-θ0)/Δθ
Δr̂

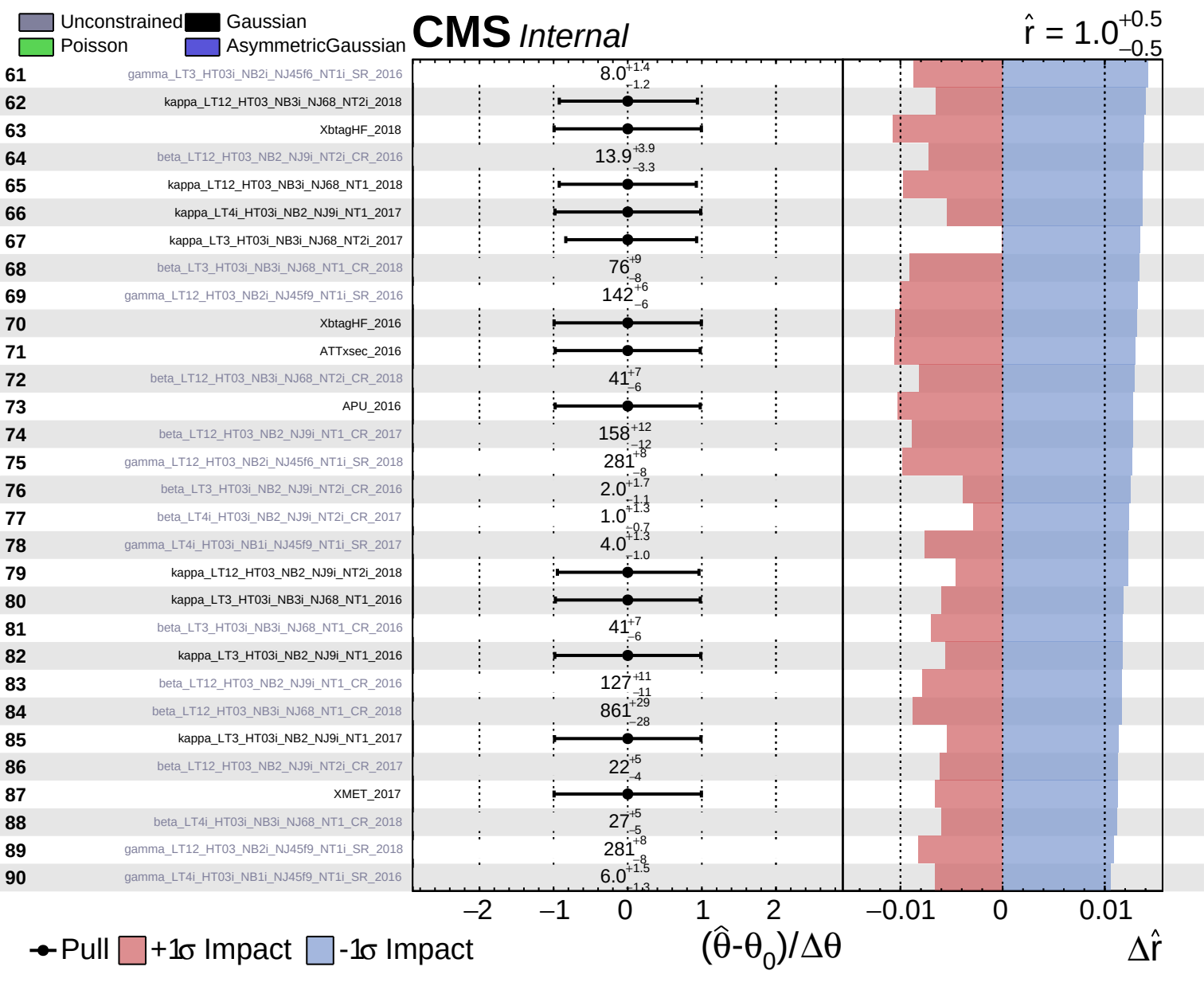
Unconstrained
Gaussian
Poisson
AsymmetricGaussian
CMS Internal
r̂ = 1.0 +0.5 −0.5
61 gamma_LT3_HT03i_NB2i_NJ45f6_NT1i_SR_2016 8.0 +1.4 −1.2
62 kappa_LT12_HT03_NB3i_NJ68_NT2i_2018
63 XbtagHF_2018
64 beta_LT12_HT03_NB2_NJ9i_NT2i_CR_2016 13.9 +3.9 −3.3
65 kappa_LT12_HT03_NB3i_NJ68_NT1_2018
66 kappa_LT4i_HT03i_NB2_NJ9i_NT1_2017
67 kappa_LT3_HT03i_NB3i_NJ68_NT2i_2017
68 beta_LT3_HT03i_NB3i_NJ68_NT1_CR_2018 76 +9 −8
69 gamma_LT12_HT03_NB2i_NJ45f9_NT1i_SR_2016 142 +6 −6
70 XbtagHF_2016
71 ATTxsec_2016
72 beta_LT12_HT03_NB3i_NJ68_NT2i_CR_2018 41 +7 −6
73 APU_2016
74 beta_LT12_HT03_NB2_NJ9i_NT1_CR_2017 158 +12 −12
75 gamma_LT12_HT03_NB2i_NJ45f6_NT1i_SR_2018 281 +8 −8
76 beta_LT3_HT03i_NB2_NJ9i_NT2i_CR_2016 2.0 +1.7 −1.1
77 beta_LT4i_HT03i_NB2_NJ9i_NT2i_CR_2017 1.0 +1.3 −0.7
78 gamma_LT4i_HT03i_NB1i_NJ45f9_NT1i_SR_2017 4.0 +1.3 −1.0
79 kappa_LT12_HT03_NB2_NJ9i_NT2i_2018
80 kappa_LT3_HT03i_NB3i_NJ68_NT1_2016
81 beta_LT3_HT03i_NB3i_NJ68_NT1_CR_2016 41 +7 −6
82 kappa_LT3_HT03i_NB2_NJ9i_NT1_2016
83 beta_LT12_HT03_NB2_NJ9i_NT1_CR_2016 127 +11 −11
84 beta_LT12_HT03_NB3i_NJ68_NT1_CR_2018 861 +29 −28
85 kappa_LT3_HT03i_NB2_NJ9i_NT1_2017
86 beta_LT12_HT03_NB2_NJ9i_NT2i_CR_2017 22 +5 −4
87 XMET_2017
88 beta_LT4i_HT03i_NB3i_NJ68_NT1_CR_2018 27 +5 −5
89 gamma_LT12_HT03_NB2i_NJ45f9_NT1i_SR_2018 281 +8 −8
90 gamma_LT4i_HT03i_NB1i_NJ45f9_NT1i_SR_2016 6.0 +1.5 −1.3
−2 −1 0 1 2
−0.01 0 0.01
Pull
+1σ Impact
-1σ Impact
(θ̂-θ0)/Δθ
Δr̂

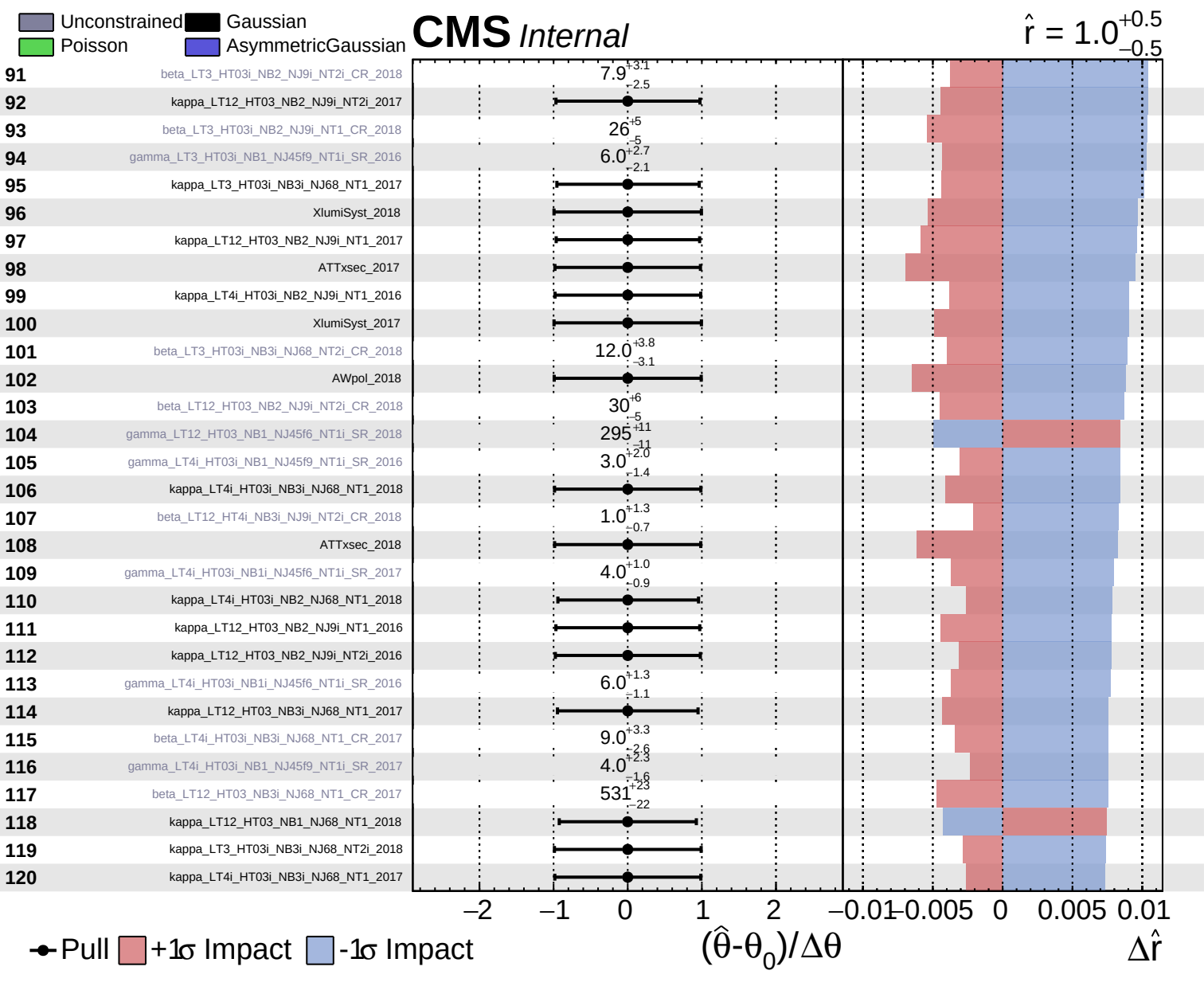
Unconstrained
Gaussian
Poisson
AsymmetricGaussian
CMS Internal
r̂ = 1.0 +0.5 −0.5
91 beta_LT3_HT03i_NB2_NJ9i_NT2i_CR_2018
92 kappa_LT12_HT03_NB2_NJ9i_NT2i_2017
93 beta_LT3_HT03i_NB2_NJ9i_NT1_CR_2018
94 gamma_LT3_HT03i_NB1_NJ45f9_NT1i_SR_2016
95 kappa_LT3_HT03i_NB3i_NJ68_NT1_2017
96 XlumiSyst_2018
97 kappa_LT12_HT03_NB2_NJ9i_NT1_2017
98 ATTxsec_2017
99 kappa_LT4i_HT03i_NB2_NJ9i_NT1_2016
100 XlumiSyst_2017
101 beta_LT3_HT03i_NB3i_NJ68_NT2i_CR_2018
102 AWpol_2018
103 beta_LT12_HT03_NB2_NJ9i_NT2i_CR_2018
104 gamma_LT12_HT03_NB1_NJ45f6_NT1i_SR_2018
105 gamma_LT4i_HT03i_NB1_NJ45f9_NT1i_SR_2016
106 kappa_LT4i_HT03i_NB3i_NJ68_NT1_2018
107 beta_LT12_HT4i_NB3i_NJ9i_NT2i_CR_2018
108 ATTxsec_2018
109 gamma_LT4i_HT03i_NB1i_NJ45f6_NT1i_SR_2017
110 kappa_LT4i_HT03i_NB2_NJ68_NT1_2018
111 kappa_LT12_HT03_NB2_NJ9i_NT1_2016
112 kappa_LT12_HT03_NB2_NJ9i_NT2i_2016
113 gamma_LT4i_HT03i_NB1i_NJ45f6_NT1i_SR_2016
114 kappa_LT12_HT03_NB3i_NJ68_NT1_2017
115 beta_LT4i_HT03i_NB3i_NJ68_NT1_CR_2017
116 gamma_LT4i_HT03i_NB1_NJ45f9_NT1i_SR_2017
117 beta_LT12_HT03_NB3i_NJ68_NT1_CR_2017
118 kappa_LT12_HT03_NB1_NJ68_NT1_2018
119 kappa_LT3_HT03i_NB3i_NJ68_NT2i_2018
120 kappa_LT4i_HT03i_NB3i_NJ68_NT1_2017
7.9 +3.1 −2.5
26 +5 −5
6.0 +2.7 −2.1
12.0 +3.8 −3.1
30 +6 −5
295 +11 −11
3.0 +2.0 −1.4
1.0 +1.3 −0.7
4.0 +1.0 −0.9
6.0 +1.3 −1.1
9.0 +3.3 −2.6
4.0 +2.3 −1.6
531 +23 −22
−2 −1 0 1 2
−0.01 −0.005 0 0.005 0.01
Pull
+1σ Impact
-1σ Impact
(θ̂-θ0)/Δθ
Δr̂

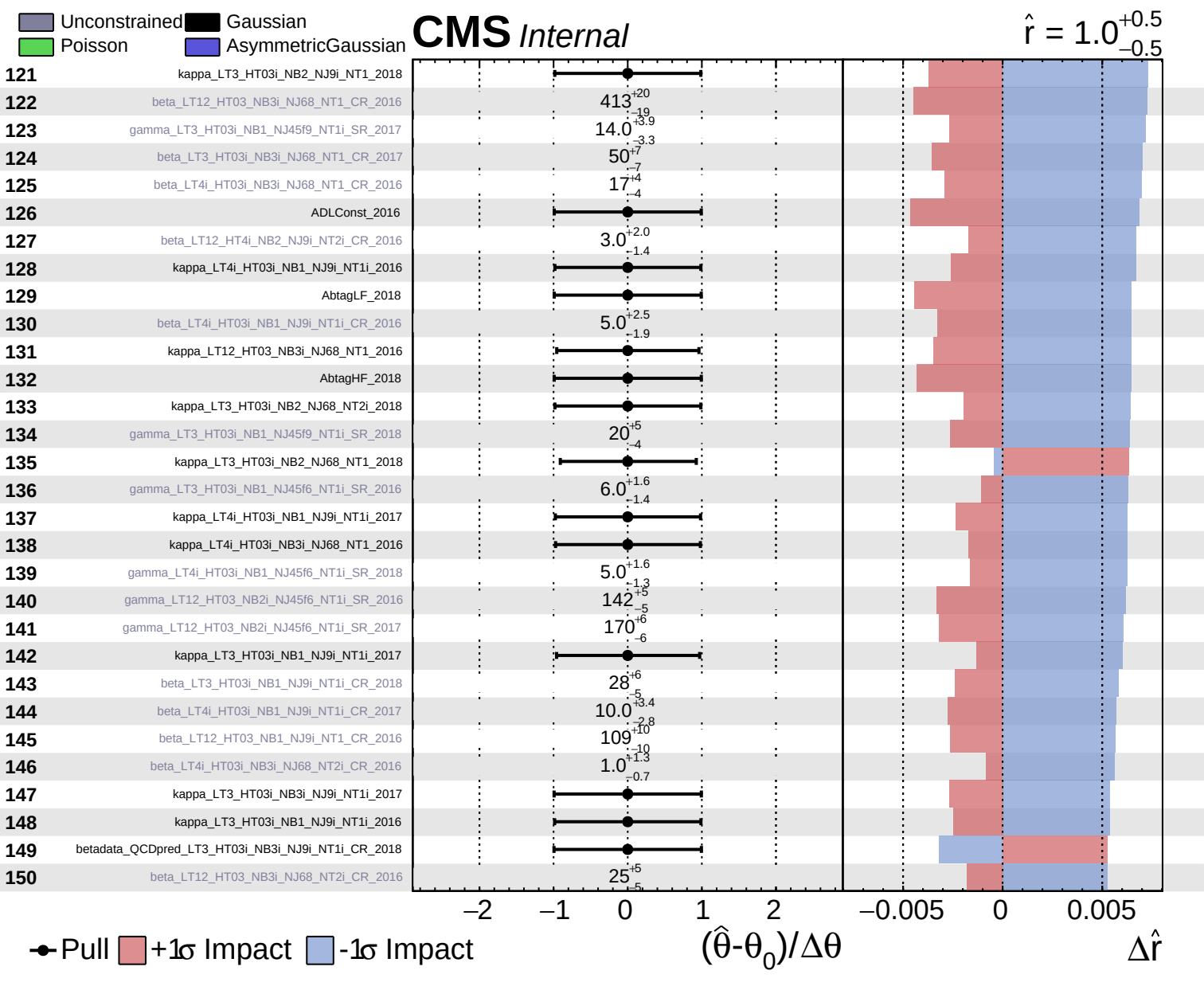
Unconstrained
Gaussian
Poisson
AsymmetricGaussian
CMS Internal
r̂ = 1.0 +0.5 −0.5
121 kappa_LT3_HT03i_NB2_NJ9i_NT1_2018
122 beta_LT12_HT03_NB3i_NJ68_NT1_CR_2016
123 gamma_LT3_HT03i_NB1_NJ45f9_NT1i_SR_2017
124 beta_LT3_HT03i_NB3i_NJ68_NT1_CR_2017
125 beta_LT4i_HT03i_NB3i_NJ68_NT1_CR_2016
126 ADLConst_2016
127 beta_LT12_HT4i_NB2_NJ9i_NT2i_CR_2016
128 kappa_LT4i_HT03i_NB1_NJ9i_NT1i_2016
129 AbtagLF_2018
130 beta_LT4i_HT03i_NB1_NJ9i_NT1i_CR_2016
131 kappa_LT12_HT03_NB3i_NJ68_NT1_2016
132 AbtagHF_2018
133 kappa_LT3_HT03i_NB2_NJ68_NT2i_2018
134 gamma_LT3_HT03i_NB1_NJ45f9_NT1i_SR_2018
135 kappa_LT3_HT03i_NB2_NJ68_NT1_2018
136 gamma_LT3_HT03i_NB1_NJ45f6_NT1i_SR_2016
137 kappa_LT4i_HT03i_NB1_NJ9i_NT1i_2017
138 kappa_LT4i_HT03i_NB3i_NJ68_NT1_2016
139 gamma_LT4i_HT03i_NB1_NJ45f6_NT1i_SR_2018
140 gamma_LT12_HT03_NB2i_NJ45f6_NT1i_SR_2016
141 gamma_LT12_HT03_NB2i_NJ45f6_NT1i_SR_2017
142 kappa_LT3_HT03i_NB1_NJ9i_NT1i_2017
143 beta_LT3_HT03i_NB1_NJ9i_NT1i_CR_2018
144 beta_LT4i_HT03i_NB1_NJ9i_NT1i_CR_2017
145 beta_LT12_HT03_NB1_NJ9i_NT1_CR_2016
146 beta_LT4i_HT03i_NB3i_NJ68_NT2i_CR_2016
147 kappa_LT3_HT03i_NB3i_NJ9i_NT1i_2017
148 kappa_LT3_HT03i_NB1_NJ9i_NT1i_2016
149 betadata_QCDpred_LT3_HT03i_NB3i_NJ9i_NT1i_CR_2018
150 beta_LT12_HT03_NB3i_NJ68_NT2i_CR_2016
413 +20 −19
14.0 +3.9 −3.3
50 +7 −7
17 +4 −4
3.0 +2.0 −1.4
5.0 +2.5 −1.9
20 +5 −4
6.0 +1.6 −1.4
5.0 +1.6 −1.3
142 +5 −5
170 +6 −6
28 +6 −5
10.0 +3.4 −2.8
109 +10 −10
1.0 +1.3 −0.7
25 +5 −5
−2
−1
0
1
2
−0.005
0
0.005
Pull
+1σ Impact
-1σ Impact
(θ̂-θ0)/Δθ
Δr̂

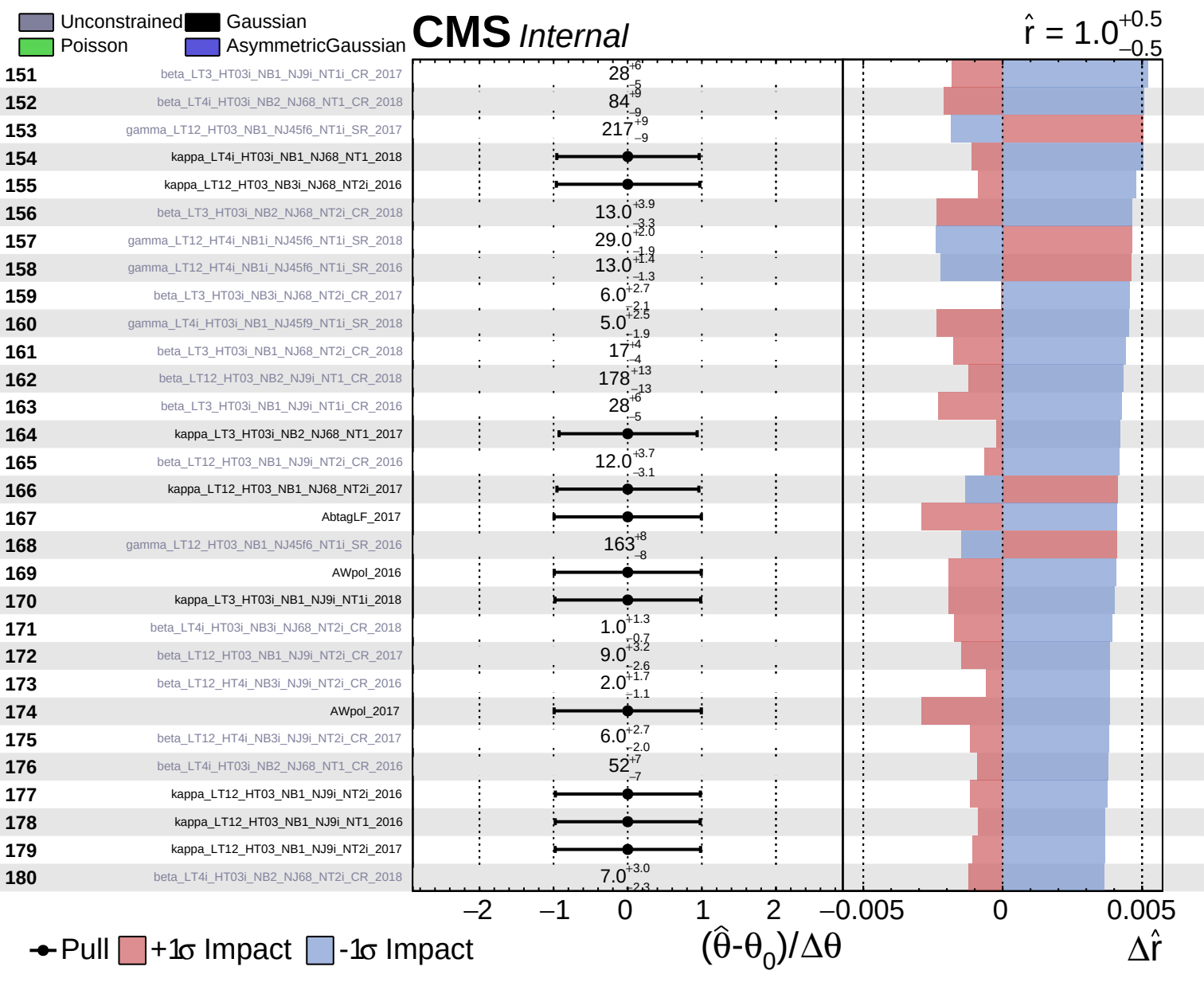
Unconstrained
Gaussian
Poisson
AsymmetricGaussian
CMS Internal
$\hat{r} = 1.0^{+0.5}_{-0.5}$
151 beta_LT3_HT03i_NB1_NJ9i_NT1i_CR_2017
152 beta_LT4i_HT03i_NB2_NJ68_NT1_CR_2018
153 gamma_LT12_HT03_NB1_NJ45f6_NT1i_SR_2017
154 kappa_LT4i_HT03i_NB1_NJ68_NT1_2018
155 kappa_LT12_HT03_NB3i_NJ68_NT2i_2016
156 beta_LT3_HT03i_NB2_NJ68_NT2i_CR_2018
157 gamma_LT12_HT4i_NB1i_NJ45f6_NT1i_SR_2018
158 gamma_LT12_HT4i_NB1i_NJ45f6_NT1i_SR_2016
159 beta_LT3_HT03i_NB3i_NJ68_NT2i_CR_2017
160 gamma_LT4i_HT03i_NB1_NJ45f9_NT1i_SR_2018
161 beta_LT3_HT03i_NB1_NJ68_NT2i_CR_2018
162 beta_LT12_HT03_NB2_NJ9i_NT1_CR_2018
163 beta_LT3_HT03i_NB1_NJ9i_NT1i_CR_2016
164 kappa_LT3_HT03i_NB2_NJ68_NT1_2017
165 beta_LT12_HT03_NB1_NJ9i_NT2i_CR_2016
166 kappa_LT12_HT03_NB1_NJ68_NT2i_2017
167 AbtagLF_2017
168 gamma_LT12_HT03_NB1_NJ45f6_NT1i_SR_2016
169 AWpol_2016
170 kappa_LT3_HT03i_NB1_NJ9i_NT1i_2018
171 beta_LT4i_HT03i_NB3i_NJ68_NT2i_CR_2018
172 beta_LT12_HT03_NB1_NJ9i_NT2i_CR_2017
173 beta_LT12_HT4i_NB3i_NJ9i_NT2i_CR_2016
174 AWpol_2017
175 beta_LT12_HT4i_NB3i_NJ9i_NT2i_CR_2017
176 beta_LT4i_HT03i_NB2_NJ68_NT1_CR_2016
177 kappa_LT12_HT03_NB1_NJ9i_NT2i_2016
178 kappa_LT12_HT03_NB1_NJ9i_NT1_2016
179 kappa_LT12_HT03_NB1_NJ9i_NT2i_2017
180 beta_LT4i_HT03i_NB2_NJ68_NT2i_CR_2018
28^{+6}_{-5}
84^{+9}_{-9}
217^{+9}_{-9}
$13.0^{+3.9}_{-3.3}$
$29.0^{+2.0}_{-1.9}$
$13.0^{+1.4}_{-1.3}$
$6.0^{+2.7}_{-2.1}$
$5.0^{+2.5}_{-1.9}$
17^{+4}_{-4}
178^{+13}_{-13}
28^{+6}_{-5}
$12.0^{+3.7}_{-3.1}$
163^{+8}_{-8}
$1.0^{+1.3}_{-0.7}$
$9.0^{+3.2}_{-2.6}$
$2.0^{+1.7}_{-1.1}$
$6.0^{+2.7}_{-2.0}$
52^{+7}_{-7}
$7.0^{+3.0}_{-2.3}$
−2
−1
0
1
2
−0.005
0
0.005
Pull
+1σ Impact
-1σ Impact
$(\hat{\theta}-\theta_0)/\Delta\theta$
$\Delta\hat{r}$

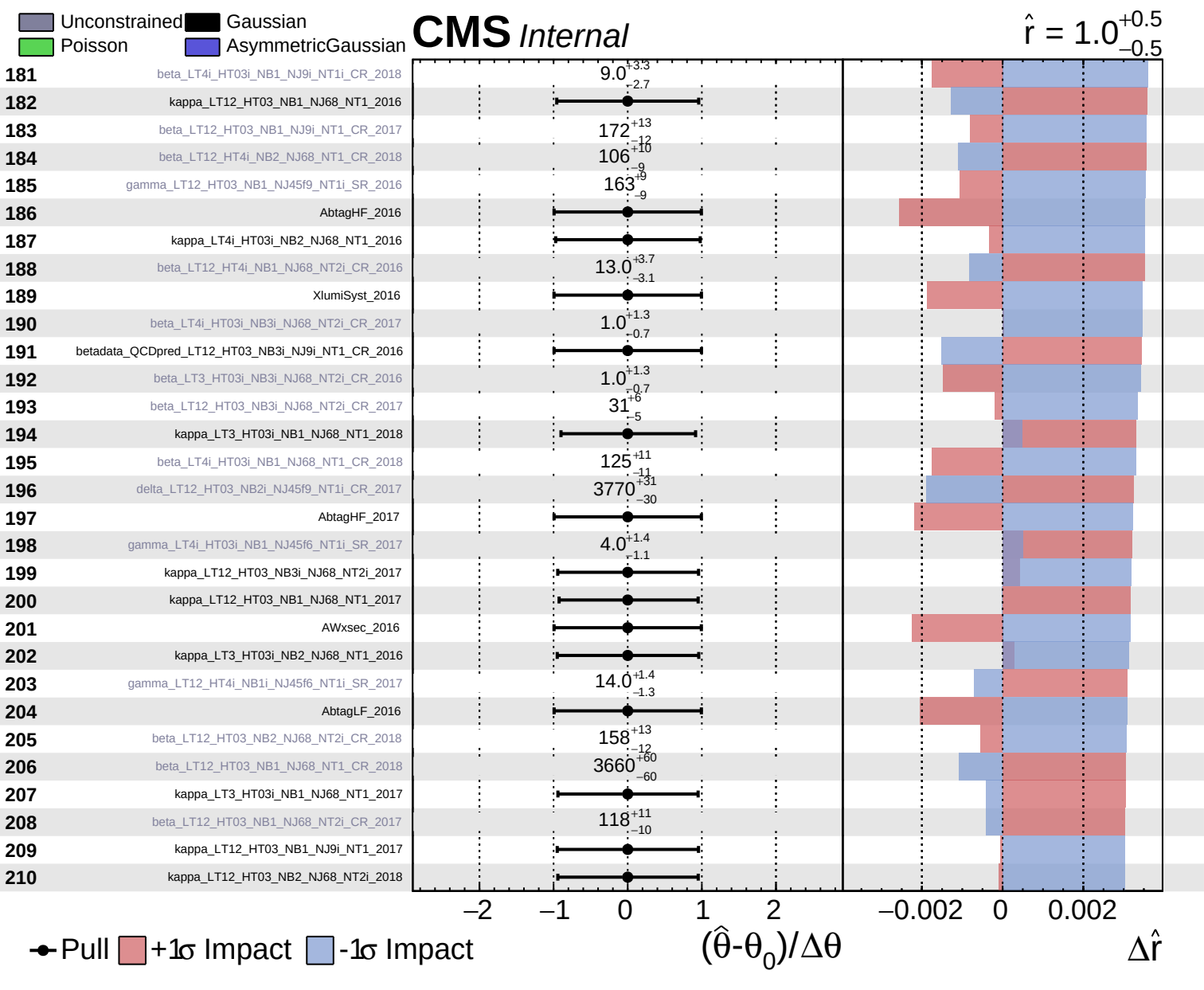
Unconstrained
Gaussian
Poisson
AsymmetricGaussian
CMS Internal
r̂ = 1.0 +0.5 −0.5
181 beta_LT4i_HT03i_NB1_NJ9i_NT1i_CR_2018
182 kappa_LT12_HT03_NB1_NJ68_NT1_2016
183 beta_LT12_HT03_NB1_NJ9i_NT1_CR_2017
184 beta_LT12_HT4i_NB2_NJ68_NT1_CR_2018
185 gamma_LT12_HT03_NB1_NJ45f9_NT1i_SR_2016
186 AbtagHF_2016
187 kappa_LT4i_HT03i_NB2_NJ68_NT1_2016
188 beta_LT12_HT4i_NB1_NJ68_NT2i_CR_2016
189 XlumiSyst_2016
190 beta_LT4i_HT03i_NB3i_NJ68_NT2i_CR_2017
191 betadata_QCDpred_LT12_HT03_NB3i_NJ9i_NT1_CR_2016
192 beta_LT3_HT03i_NB3i_NJ68_NT2i_CR_2016
193 beta_LT12_HT03_NB3i_NJ68_NT2i_CR_2017
194 kappa_LT3_HT03i_NB1_NJ68_NT1_2018
195 beta_LT4i_HT03i_NB1_NJ68_NT1_CR_2018
196 delta_LT12_HT03_NB2i_NJ45f9_NT1i_CR_2017
197 AbtagHF_2017
198 gamma_LT4i_HT03i_NB1_NJ45f6_NT1i_SR_2017
199 kappa_LT12_HT03_NB3i_NJ68_NT2i_2017
200 kappa_LT12_HT03_NB1_NJ68_NT1_2017
201 AWxsec_2016
202 kappa_LT3_HT03i_NB2_NJ68_NT1_2016
203 gamma_LT12_HT4i_NB1i_NJ45f6_NT1i_SR_2017
204 AbtagLF_2016
205 beta_LT12_HT03_NB2_NJ68_NT2i_CR_2018
206 beta_LT12_HT03_NB1_NJ68_NT1_CR_2018
207 kappa_LT3_HT03i_NB1_NJ68_NT1_2017
208 beta_LT12_HT03_NB1_NJ68_NT2i_CR_2017
209 kappa_LT12_HT03_NB1_NJ9i_NT1_2017
210 kappa_LT12_HT03_NB2_NJ68_NT2i_2018
9.0 +3.3 −2.7
172 +13 −12
106 +10 −9
163 +9 −9
13.0 +3.7 −3.1
1.0 +1.3 −0.7
1.0 +1.3 −0.7
31 +6 −5
125 +11 −11
3770 +31 −30
4.0 +1.4 −1.1
14.0 +1.4 −1.3
158 +13 −12
3660 +60 −60
118 +11 −10
−2
−1
0
1
2
−0.002
0
0.002
Pull
+1σ Impact
-1σ Impact
(θ̂-θ0)/Δθ
Δr̂

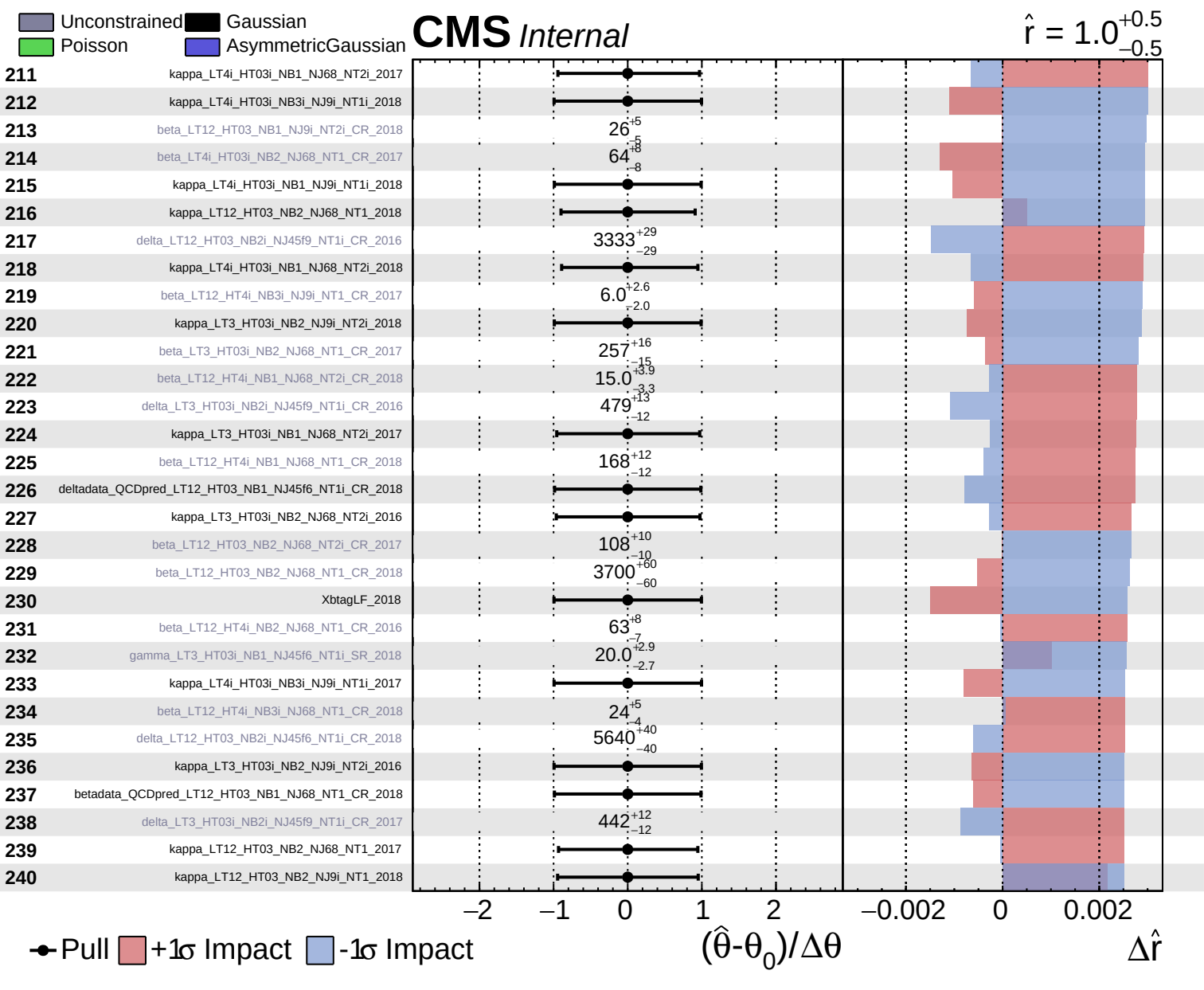
Unconstrained
Gaussian
Poisson
AsymmetricGaussian
CMS Internal
$\hat{r} = 1.0^{+0.5}_{-0.5}$
211 kappa_LT4i_HT03i_NB1_NJ68_NT2i_2017
212 kappa_LT4i_HT03i_NB3i_NJ9i_NT1i_2018
213 beta_LT12_HT03_NB1_NJ9i_NT2i_CR_2018
214 beta_LT4i_HT03i_NB2_NJ68_NT1_CR_2017
215 kappa_LT4i_HT03i_NB1_NJ9i_NT1i_2018
216 kappa_LT12_HT03_NB2_NJ68_NT1_2018
217 delta_LT12_HT03_NB2i_NJ45f9_NT1i_CR_2016
218 kappa_LT4i_HT03i_NB1_NJ68_NT2i_2018
219 beta_LT12_HT4i_NB3i_NJ9i_NT1_CR_2017
220 kappa_LT3_HT03i_NB2_NJ9i_NT2i_2018
221 beta_LT3_HT03i_NB2_NJ68_NT1_CR_2017
222 beta_LT12_HT4i_NB1_NJ68_NT2i_CR_2018
223 delta_LT3_HT03i_NB2i_NJ45f9_NT1i_CR_2016
224 kappa_LT3_HT03i_NB1_NJ68_NT2i_2017
225 beta_LT12_HT4i_NB1_NJ68_NT1_CR_2018
226 deltadata_QCDpred_LT12_HT03_NB1_NJ45f6_NT1i_CR_2018
227 kappa_LT3_HT03i_NB2_NJ68_NT2i_2016
228 beta_LT12_HT03_NB2_NJ68_NT2i_CR_2017
229 beta_LT12_HT03_NB2_NJ68_NT1_CR_2018
230 XbtagLF_2018
231 beta_LT12_HT4i_NB2_NJ68_NT1_CR_2016
232 gamma_LT3_HT03i_NB1_NJ45f6_NT1i_SR_2018
233 kappa_LT4i_HT03i_NB3i_NJ9i_NT1i_2017
234 beta_LT12_HT4i_NB3i_NJ68_NT1_CR_2018
235 delta_LT12_HT03_NB2i_NJ45f6_NT1i_CR_2018
236 kappa_LT3_HT03i_NB2_NJ9i_NT2i_2016
237 betadata_QCDpred_LT12_HT03_NB1_NJ68_NT1_CR_2018
238 delta_LT3_HT03i_NB2i_NJ45f9_NT1i_CR_2017
239 kappa_LT12_HT03_NB2_NJ68_NT1_2017
240 kappa_LT12_HT03_NB2_NJ9i_NT1_2018
26^{+5}_{-5}
64^{+8}_{-8}
3333^{+29}_{-29}
$6.0^{+2.6}_{-2.0}$
257^{+16}_{-15}
$15.0^{+3.9}_{-3.3}$
479^{+13}_{-12}
168^{+12}_{-12}
108^{+10}_{-10}
3700^{+60}_{-60}
63^{+8}_{-7}
$20.0^{+2.9}_{-2.7}$
24^{+5}_{-4}
5640^{+40}_{-40}
442^{+12}_{-12}
−2
−1
0
1
2
−0.002
0
0.002
Pull
+1σ Impact
-1σ Impact
$(\hat{\theta}-\theta_0)/\Delta\theta$
$\Delta\hat{r}$

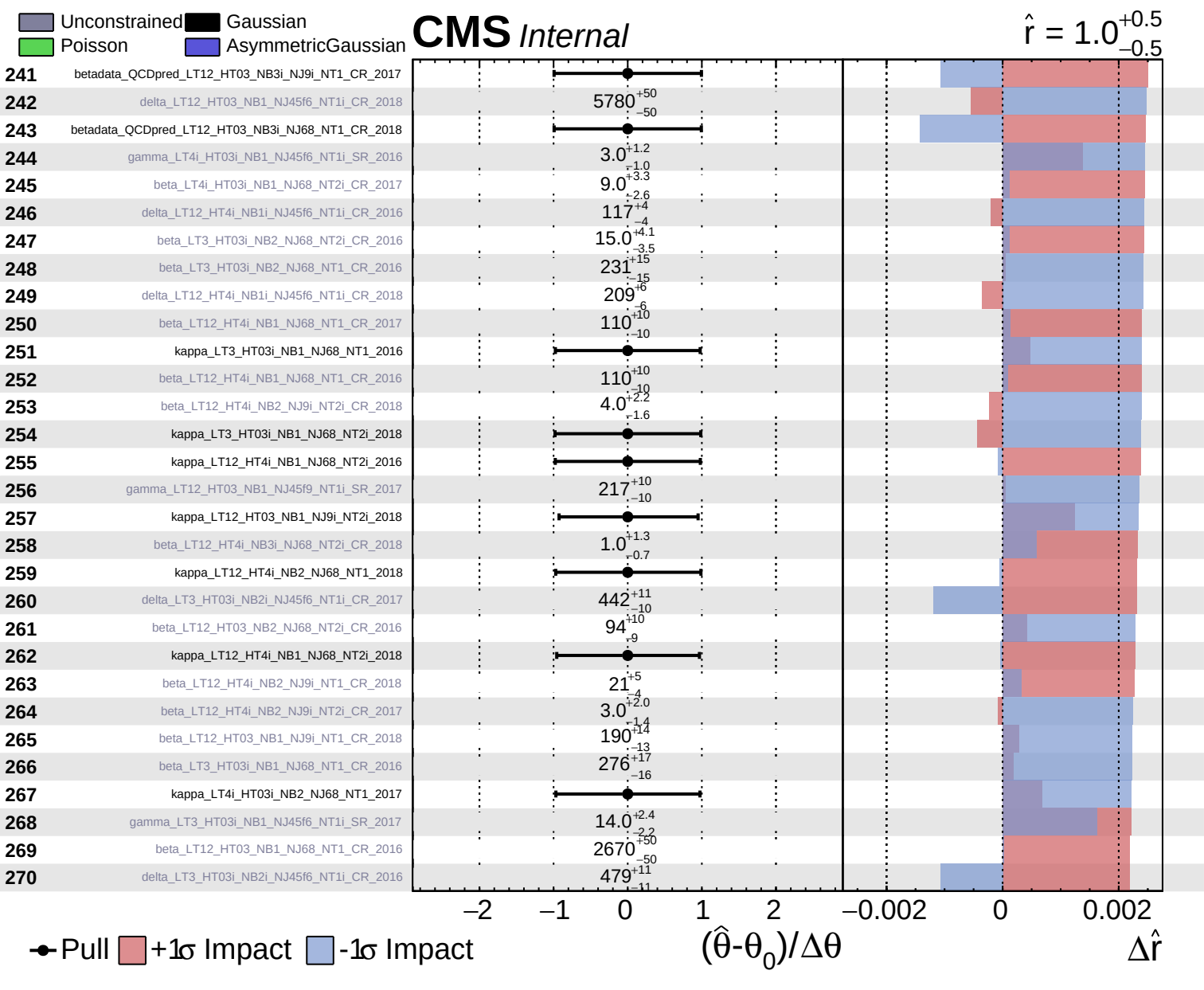
Unconstrained
Gaussian
Poisson
AsymmetricGaussian
CMS Internal
r̂ = 1.0 +0.5 −0.5
241 betadata_QCDpred_LT12_HT03_NB3i_NJ9i_NT1_CR_2017
242 delta_LT12_HT03_NB1_NJ45f6_NT1i_CR_2018
5780 +50 −50
243 betadata_QCDpred_LT12_HT03_NB3i_NJ68_NT1_CR_2018
244 gamma_LT4i_HT03i_NB1_NJ45f6_NT1i_SR_2016
3.0 +1.2 −1.0
245 beta_LT4i_HT03i_NB1_NJ68_NT2i_CR_2017
9.0 +3.3 −2.6
246 delta_LT12_HT4i_NB1i_NJ45f6_NT1i_CR_2016
117 +4 −4
247 beta_LT3_HT03i_NB2_NJ68_NT2i_CR_2016
15.0 +4.1 −3.5
248 beta_LT3_HT03i_NB2_NJ68_NT1_CR_2016
231 +15 −15
249 delta_LT12_HT4i_NB1i_NJ45f6_NT1i_CR_2018
209 +6 −6
250 beta_LT12_HT4i_NB1_NJ68_NT1_CR_2017
110 +10 −10
251 kappa_LT3_HT03i_NB1_NJ68_NT1_2016
252 beta_LT12_HT4i_NB1_NJ68_NT1_CR_2016
110 +10 −10
253 beta_LT12_HT4i_NB2_NJ9i_NT2i_CR_2018
4.0 +2.2 −1.6
254 kappa_LT3_HT03i_NB1_NJ68_NT2i_2018
255 kappa_LT12_HT4i_NB1_NJ68_NT2i_2016
256 gamma_LT12_HT03_NB1_NJ45f9_NT1i_SR_2017
217 +10 −10
257 kappa_LT12_HT03_NB1_NJ9i_NT2i_2018
258 beta_LT12_HT4i_NB3i_NJ68_NT2i_CR_2018
1.0 +1.3 −0.7
259 kappa_LT12_HT4i_NB2_NJ68_NT1_2018
260 delta_LT3_HT03i_NB2i_NJ45f6_NT1i_CR_2017
442 +11 −10
261 beta_LT12_HT03_NB2_NJ68_NT2i_CR_2016
94 +10 −9
262 kappa_LT12_HT4i_NB1_NJ68_NT2i_2018
263 beta_LT12_HT4i_NB2_NJ9i_NT1_CR_2018
21 +5 −4
264 beta_LT12_HT4i_NB2_NJ9i_NT2i_CR_2017
3.0 +2.0 −1.4
265 beta_LT12_HT03_NB1_NJ9i_NT1_CR_2018
190 +14 −13
266 beta_LT3_HT03i_NB1_NJ68_NT1_CR_2016
276 +17 −16
267 kappa_LT4i_HT03i_NB2_NJ68_NT1_2017
268 gamma_LT3_HT03i_NB1_NJ45f6_NT1i_SR_2017
14.0 +2.4 −2.2
269 beta_LT12_HT03_NB1_NJ68_NT1_CR_2016
2670 +50 −50
270 delta_LT3_HT03i_NB2i_NJ45f6_NT1i_CR_2016
479 +11 −11
−2 −1 0 1 2
−0.002 0 0.002
Pull
+1σ Impact
-1σ Impact
(θ̂-θ0)/Δθ
Δr̂

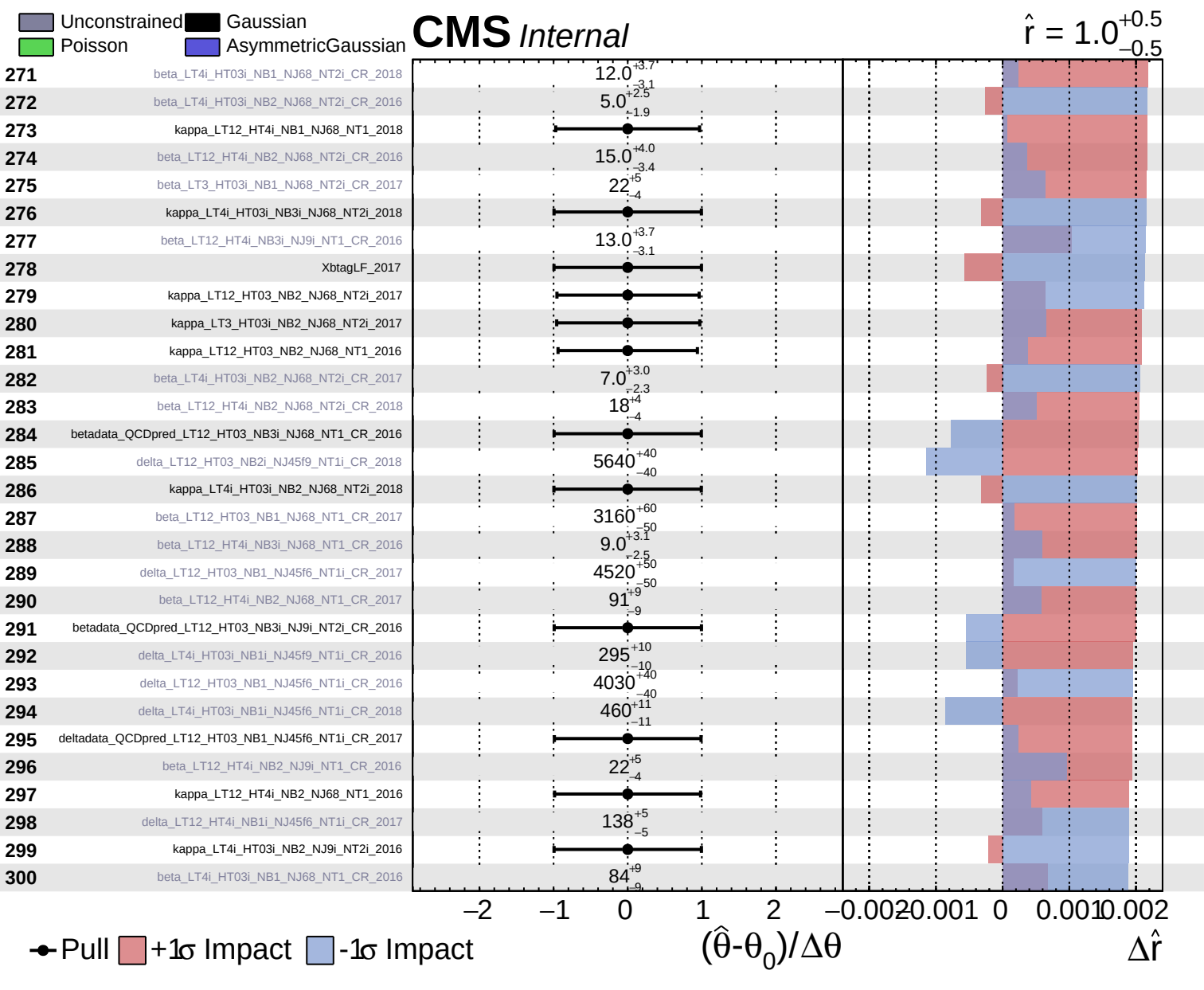
Unconstrained
Gaussian
Poisson
AsymmetricGaussian
CMS Internal
r̂ = 1.0 +0.5 −0.5
271 beta_LT4i_HT03i_NB1_NJ68_NT2i_CR_2018
272 beta_LT4i_HT03i_NB2_NJ68_NT2i_CR_2016
273 kappa_LT12_HT4i_NB1_NJ68_NT1_2018
274 beta_LT12_HT4i_NB2_NJ68_NT2i_CR_2016
275 beta_LT3_HT03i_NB1_NJ68_NT2i_CR_2017
276 kappa_LT4i_HT03i_NB3i_NJ68_NT2i_2018
277 beta_LT12_HT4i_NB3i_NJ9i_NT1_CR_2016
278 XbtagLF_2017
279 kappa_LT12_HT03_NB2_NJ68_NT2i_2017
280 kappa_LT3_HT03i_NB2_NJ68_NT2i_2017
281 kappa_LT12_HT03_NB2_NJ68_NT1_2016
282 beta_LT4i_HT03i_NB2_NJ68_NT2i_CR_2017
283 beta_LT12_HT4i_NB2_NJ68_NT2i_CR_2018
284 betadata_QCDpred_LT12_HT03_NB3i_NJ68_NT1_CR_2016
285 delta_LT12_HT03_NB2i_NJ45f9_NT1i_CR_2018
286 kappa_LT4i_HT03i_NB2_NJ68_NT2i_2018
287 beta_LT12_HT03_NB1_NJ68_NT1_CR_2017
288 beta_LT12_HT4i_NB3i_NJ68_NT1_CR_2016
289 delta_LT12_HT03_NB1_NJ45f6_NT1i_CR_2017
290 beta_LT12_HT4i_NB2_NJ68_NT1_CR_2017
291 betadata_QCDpred_LT12_HT03_NB3i_NJ9i_NT2i_CR_2016
292 delta_LT4i_HT03i_NB1i_NJ45f9_NT1i_CR_2016
293 delta_LT12_HT03_NB1_NJ45f6_NT1i_CR_2016
294 delta_LT4i_HT03i_NB1i_NJ45f6_NT1i_CR_2018
295 deltadata_QCDpred_LT12_HT03_NB1_NJ45f6_NT1i_CR_2017
296 beta_LT12_HT4i_NB2_NJ9i_NT1_CR_2016
297 kappa_LT12_HT4i_NB2_NJ68_NT1_2016
298 delta_LT12_HT4i_NB1i_NJ45f6_NT1i_CR_2017
299 kappa_LT4i_HT03i_NB2_NJ9i_NT2i_2016
300 beta_LT4i_HT03i_NB1_NJ68_NT1_CR_2016
12.0 +3.7 −3.1
5.0 +2.5 −1.9
15.0 +4.0 −3.4
22 +5 −4
13.0 +3.7 −3.1
7.0 +3.0 −2.3
18 +4 −4
5640 +40 −40
3160 +60 −50
9.0 +3.1 −2.5
4520 +50 −50
91 +9 −9
295 +10 −10
4030 +40 −40
460 +11 −11
22 +5 −4
138 +5 −5
84 +9 −9
−2
−1
0
1
2
−0.002
−0.001
0
0.001
0.002
Pull
+1σ Impact
-1σ Impact
(θ̂-θ0)/Δθ
Δr̂

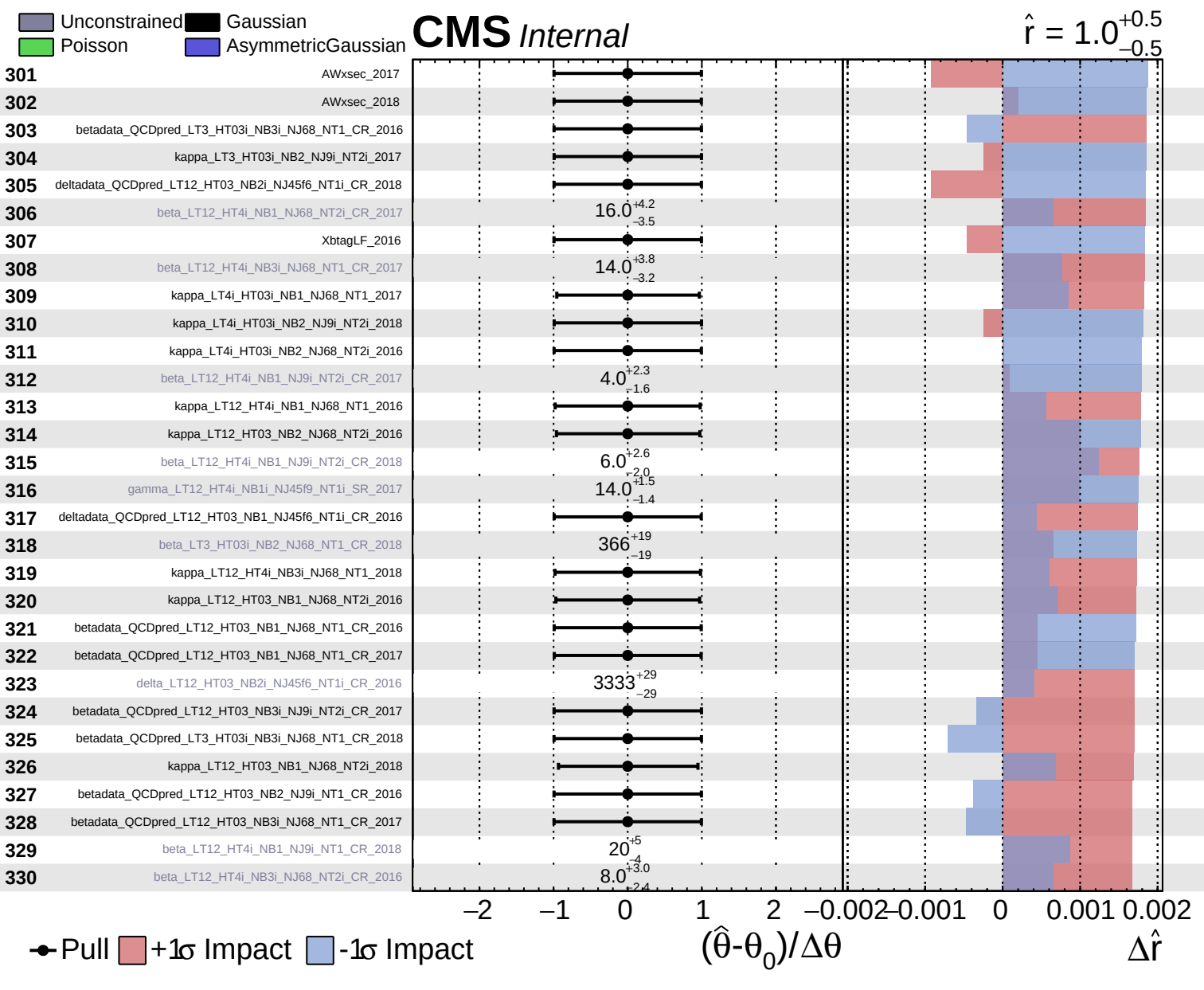
Unconstrained
Gaussian
Poisson
AsymmetricGaussian
CMS Internal
$\hat{r} = 1.0^{+0.5}_{-0.5}$
301 AWxsec_2017
302 AWxsec_2018
303 betadata_QCDpred_LT3_HT03i_NB3i_NJ68_NT1_CR_2016
304 kappa_LT3_HT03i_NB2_NJ9i_NT2i_2017
305 deltadata_QCDpred_LT12_HT03_NB2i_NJ45f6_NT1i_CR_2018
306 beta_LT12_HT4i_NB1_NJ68_NT2i_CR_2017
$16.0^{+4.2}_{-3.5}$
307 XbtagLF_2016
308 beta_LT12_HT4i_NB3i_NJ68_NT1_CR_2017
$14.0^{+3.8}_{-3.2}$
309 kappa_LT4i_HT03i_NB1_NJ68_NT1_2017
310 kappa_LT4i_HT03i_NB2_NJ9i_NT2i_2018
311 kappa_LT4i_HT03i_NB2_NJ68_NT2i_2016
312 beta_LT12_HT4i_NB1_NJ9i_NT2i_CR_2017
$4.0^{+2.3}_{-1.6}$
313 kappa_LT12_HT4i_NB1_NJ68_NT1_2016
314 kappa_LT12_HT03_NB2_NJ68_NT2i_2016
315 beta_LT12_HT4i_NB1_NJ9i_NT2i_CR_2018
$6.0^{+2.6}_{-2.0}$
316 gamma_LT12_HT4i_NB1i_NJ45f9_NT1i_SR_2017
$14.0^{+1.5}_{-1.4}$
317 deltadata_QCDpred_LT12_HT03_NB1_NJ45f6_NT1i_CR_2016
318 beta_LT3_HT03i_NB2_NJ68_NT1_CR_2018
366^{+19}_{-19}
319 kappa_LT12_HT4i_NB3i_NJ68_NT1_2018
320 kappa_LT12_HT03_NB1_NJ68_NT2i_2016
321 betadata_QCDpred_LT12_HT03_NB1_NJ68_NT1_CR_2016
322 betadata_QCDpred_LT12_HT03_NB1_NJ68_NT1_CR_2017
323 delta_LT12_HT03_NB2i_NJ45f6_NT1i_CR_2016
3333^{+29}_{-29}
324 betadata_QCDpred_LT12_HT03_NB3i_NJ9i_NT2i_CR_2017
325 betadata_QCDpred_LT3_HT03i_NB3i_NJ68_NT1_CR_2018
326 kappa_LT12_HT03_NB1_NJ68_NT2i_2018
327 betadata_QCDpred_LT12_HT03_NB2_NJ9i_NT1_CR_2016
328 betadata_QCDpred_LT12_HT03_NB3i_NJ68_NT1_CR_2017
329 beta_LT12_HT4i_NB1_NJ9i_NT1_CR_2018
20^{+5}_{-4}
330 beta_LT12_HT4i_NB3i_NJ68_NT2i_CR_2016
$8.0^{+3.0}_{-2.4}$
−2 −1 0 1 2
−0.002 −0.001 0 0.001 0.002
Pull
+1σ Impact
-1σ Impact
$(\hat{\theta}-\theta_0)/\Delta\theta$
$\Delta\hat{r}$

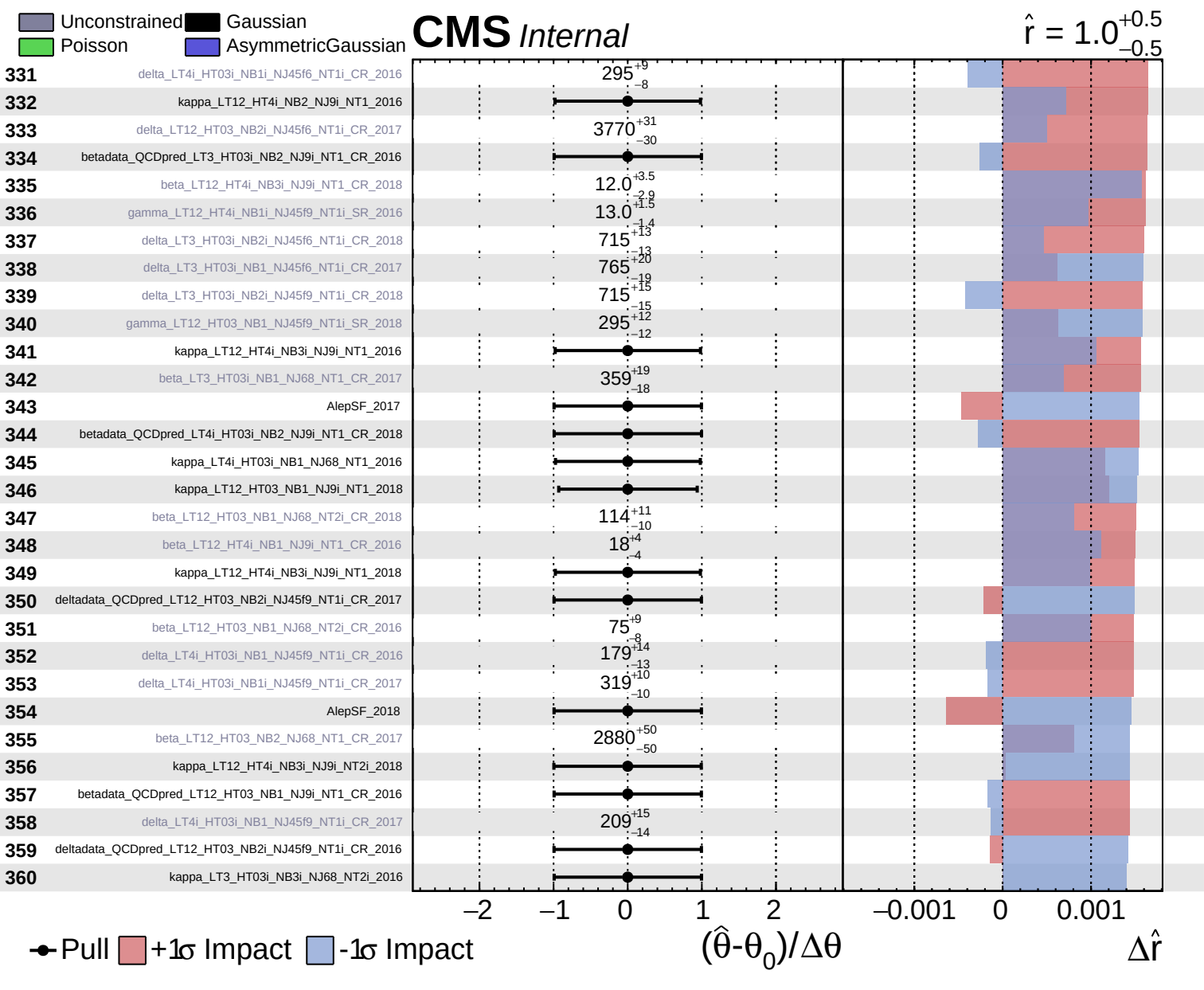
Unconstrained
Gaussian
Poisson
AsymmetricGaussian
CMS Internal
r̂ = 1.0 +0.5 −0.5
331 delta_LT4i_HT03i_NB1i_NJ45f6_NT1i_CR_2016
332 kappa_LT12_HT4i_NB2_NJ9i_NT1_2016
333 delta_LT12_HT03_NB2i_NJ45f6_NT1i_CR_2017
334 betadata_QCDpred_LT3_HT03i_NB2_NJ9i_NT1_CR_2016
335 beta_LT12_HT4i_NB3i_NJ9i_NT1_CR_2018
336 gamma_LT12_HT4i_NB1i_NJ45f9_NT1i_SR_2016
337 delta_LT3_HT03i_NB2i_NJ45f6_NT1i_CR_2018
338 delta_LT3_HT03i_NB1_NJ45f6_NT1i_CR_2017
339 delta_LT3_HT03i_NB2i_NJ45f9_NT1i_CR_2018
340 gamma_LT12_HT03_NB1_NJ45f9_NT1i_SR_2018
341 kappa_LT12_HT4i_NB3i_NJ9i_NT1_2016
342 beta_LT3_HT03i_NB1_NJ68_NT1_CR_2017
343 AlepSF_2017
344 betadata_QCDpred_LT4i_HT03i_NB2_NJ9i_NT1_CR_2018
345 kappa_LT4i_HT03i_NB1_NJ68_NT1_2016
346 kappa_LT12_HT03_NB1_NJ9i_NT1_2018
347 beta_LT12_HT03_NB1_NJ68_NT2i_CR_2018
348 beta_LT12_HT4i_NB1_NJ9i_NT1_CR_2016
349 kappa_LT12_HT4i_NB3i_NJ9i_NT1_2018
350 deltadata_QCDpred_LT12_HT03_NB2i_NJ45f9_NT1i_CR_2017
351 beta_LT12_HT03_NB1_NJ68_NT2i_CR_2016
352 delta_LT4i_HT03i_NB1_NJ45f9_NT1i_CR_2016
353 delta_LT4i_HT03i_NB1i_NJ45f9_NT1i_CR_2017
354 AlepSF_2018
355 beta_LT12_HT03_NB2_NJ68_NT1_CR_2017
356 kappa_LT12_HT4i_NB3i_NJ9i_NT2i_2018
357 betadata_QCDpred_LT12_HT03_NB1_NJ9i_NT1_CR_2016
358 delta_LT4i_HT03i_NB1_NJ45f9_NT1i_CR_2017
359 deltadata_QCDpred_LT12_HT03_NB2i_NJ45f9_NT1i_CR_2016
360 kappa_LT3_HT03i_NB3i_NJ68_NT2i_2016
295 +9 −8
3770 +31 −30
12.0 +3.5 −2.9
13.0 +1.5 −1.4
715 +13 −13
765 +20 −19
715 +15 −15
295 +12 −12
359 +19 −18
114 +11 −10
18 +4 −4
75 +9 −8
179 +14 −13
319 +10 −10
2880 +50 −50
209 +15 −14
−2
−1
0
1
2
−0.001
0
0.001
Pull
+1σ Impact
-1σ Impact
(θ̂-θ0)/Δθ
Δr̂

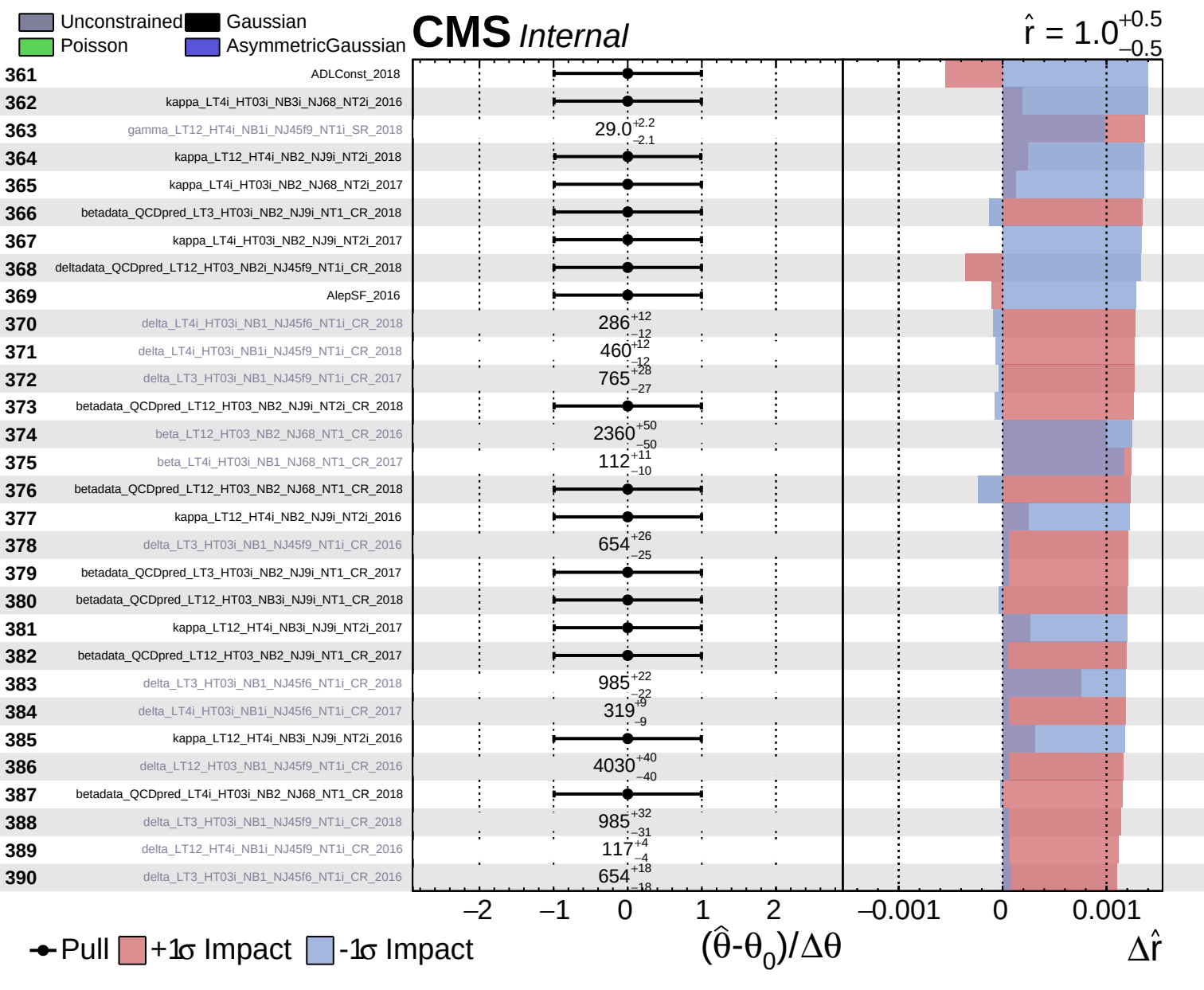
Unconstrained
Gaussian
Poisson
AsymmetricGaussian
CMS Internal
r̂ = 1.0 +0.5 −0.5
361 ADLConst_2018
362 kappa_LT4i_HT03i_NB3i_NJ68_NT2i_2016
363 gamma_LT12_HT4i_NB1i_NJ45f9_NT1i_SR_2018
29.0 +2.2 −2.1
364 kappa_LT12_HT4i_NB2_NJ9i_NT2i_2018
365 kappa_LT4i_HT03i_NB2_NJ68_NT2i_2017
366 betadata_QCDpred_LT3_HT03i_NB2_NJ9i_NT1_CR_2018
367 kappa_LT4i_HT03i_NB2_NJ9i_NT2i_2017
368 deltadata_QCDpred_LT12_HT03_NB2i_NJ45f9_NT1i_CR_2018
369 AlepSF_2016
370 delta_LT4i_HT03i_NB1_NJ45f6_NT1i_CR_2018
286 +12 −12
371 delta_LT4i_HT03i_NB1_NJ45f9_NT1i_CR_2018
460 +12 −12
372 delta_LT3_HT03i_NB1_NJ45f9_NT1i_CR_2017
765 +28 −27
373 betadata_QCDpred_LT12_HT03_NB2_NJ9i_NT2i_CR_2018
374 beta_LT12_HT03_NB2_NJ68_NT1_CR_2016
2360 +50 −50
375 beta_LT4i_HT03i_NB1_NJ68_NT1_CR_2017
112 +11 −10
376 betadata_QCDpred_LT12_HT03_NB2_NJ68_NT1_CR_2018
377 kappa_LT12_HT4i_NB2_NJ9i_NT2i_2016
378 delta_LT3_HT03i_NB1_NJ45f9_NT1i_CR_2016
654 +26 −25
379 betadata_QCDpred_LT3_HT03i_NB2_NJ9i_NT1_CR_2017
380 betadata_QCDpred_LT12_HT03_NB3i_NJ9i_NT1_CR_2018
381 kappa_LT12_HT4i_NB3i_NJ9i_NT2i_2017
382 betadata_QCDpred_LT12_HT03_NB2_NJ9i_NT1_CR_2017
383 delta_LT3_HT03i_NB1_NJ45f6_NT1i_CR_2018
985 +22 −22
384 delta_LT4i_HT03i_NB1i_NJ45f6_NT1i_CR_2017
319 +9 −9
385 kappa_LT12_HT4i_NB3i_NJ9i_NT2i_2016
386 delta_LT12_HT03_NB1_NJ45f9_NT1i_CR_2016
4030 +40 −40
387 betadata_QCDpred_LT4i_HT03i_NB2_NJ68_NT1_CR_2018
388 delta_LT3_HT03i_NB1_NJ45f9_NT1i_CR_2018
985 +32 −31
389 delta_LT12_HT4i_NB1i_NJ45f9_NT1i_CR_2016
117 +4 −4
390 delta_LT3_HT03i_NB1_NJ45f6_NT1i_CR_2016
654 +18 −18
−2 −1 0 1 2
−0.001 0 0.001
Pull
+1σ Impact
-1σ Impact
(θ̂-θ0)/Δθ
Δr̂

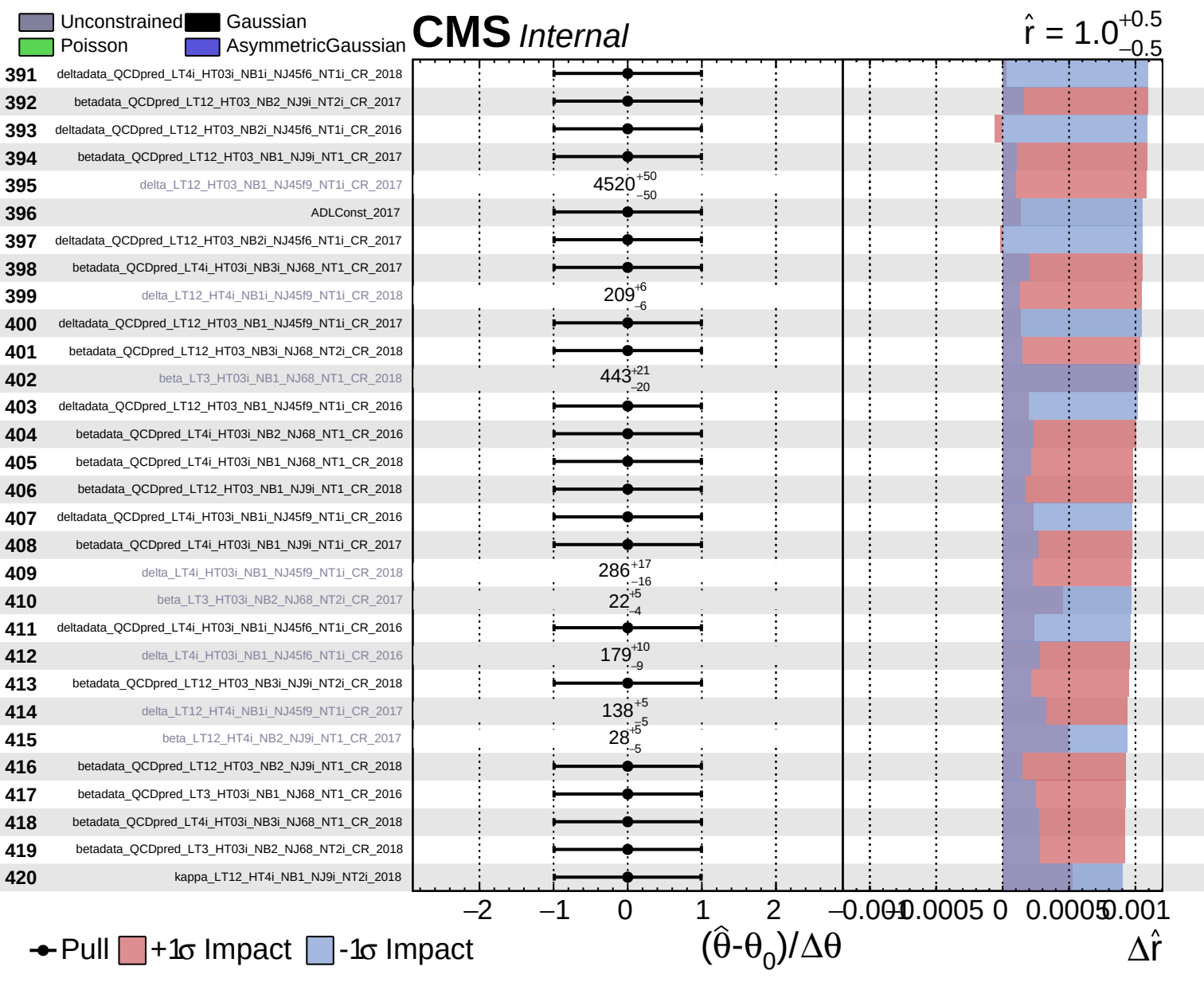
Unconstrained
Gaussian
Poisson
AsymmetricGaussian
CMS Internal
r̂ = 1.0 +0.5 −0.5
391 deltadata_QCDpred_LT4i_HT03i_NB1i_NJ45f6_NT1i_CR_2018
392 betadata_QCDpred_LT12_HT03_NB2_NJ9i_NT2i_CR_2017
393 deltadata_QCDpred_LT12_HT03_NB2i_NJ45f6_NT1i_CR_2016
394 betadata_QCDpred_LT12_HT03_NB1_NJ9i_NT1_CR_2017
395 delta_LT12_HT03_NB1_NJ45f9_NT1i_CR_2017
4520 +50 −50
396 ADLConst_2017
397 deltadata_QCDpred_LT12_HT03_NB2i_NJ45f6_NT1i_CR_2017
398 betadata_QCDpred_LT4i_HT03i_NB3i_NJ68_NT1_CR_2017
399 delta_LT12_HT4i_NB1i_NJ45f9_NT1i_CR_2018
209 +6 −6
400 deltadata_QCDpred_LT12_HT03_NB1_NJ45f9_NT1i_CR_2017
401 betadata_QCDpred_LT12_HT03_NB3i_NJ68_NT2i_CR_2018
402 beta_LT3_HT03i_NB1_NJ68_NT1_CR_2018
443 +21 −20
403 deltadata_QCDpred_LT12_HT03_NB1_NJ45f9_NT1i_CR_2016
404 betadata_QCDpred_LT4i_HT03i_NB2_NJ68_NT1_CR_2016
405 betadata_QCDpred_LT4i_HT03i_NB1_NJ68_NT1_CR_2018
406 betadata_QCDpred_LT12_HT03_NB1_NJ9i_NT1_CR_2018
407 deltadata_QCDpred_LT4i_HT03i_NB1i_NJ45f9_NT1i_CR_2016
408 betadata_QCDpred_LT4i_HT03i_NB1_NJ9i_NT1i_CR_2017
409 delta_LT4i_HT03i_NB1_NJ45f9_NT1i_CR_2018
286 +17 −16
410 beta_LT3_HT03i_NB2_NJ68_NT2i_CR_2017
22 +5 −4
411 deltadata_QCDpred_LT4i_HT03i_NB1i_NJ45f6_NT1i_CR_2016
412 delta_LT4i_HT03i_NB1_NJ45f6_NT1i_CR_2016
179 +10 −9
413 betadata_QCDpred_LT12_HT03_NB3i_NJ9i_NT2i_CR_2018
414 delta_LT12_HT4i_NB1i_NJ45f9_NT1i_CR_2017
138 +5 −5
415 beta_LT12_HT4i_NB2_NJ9i_NT1_CR_2017
28 +5 −5
416 betadata_QCDpred_LT12_HT03_NB2_NJ9i_NT1_CR_2018
417 betadata_QCDpred_LT3_HT03i_NB1_NJ68_NT1_CR_2016
418 betadata_QCDpred_LT4i_HT03i_NB3i_NJ68_NT1_CR_2018
419 betadata_QCDpred_LT3_HT03i_NB2_NJ68_NT2i_CR_2018
420 kappa_LT12_HT4i_NB1_NJ9i_NT2i_2018
−2 −1 0 1 2
−0.001 −0.0005 0 0.0005 0.001
Pull +1σ Impact -1σ Impact
(θ̂-θ0)/Δθ
Δr̂

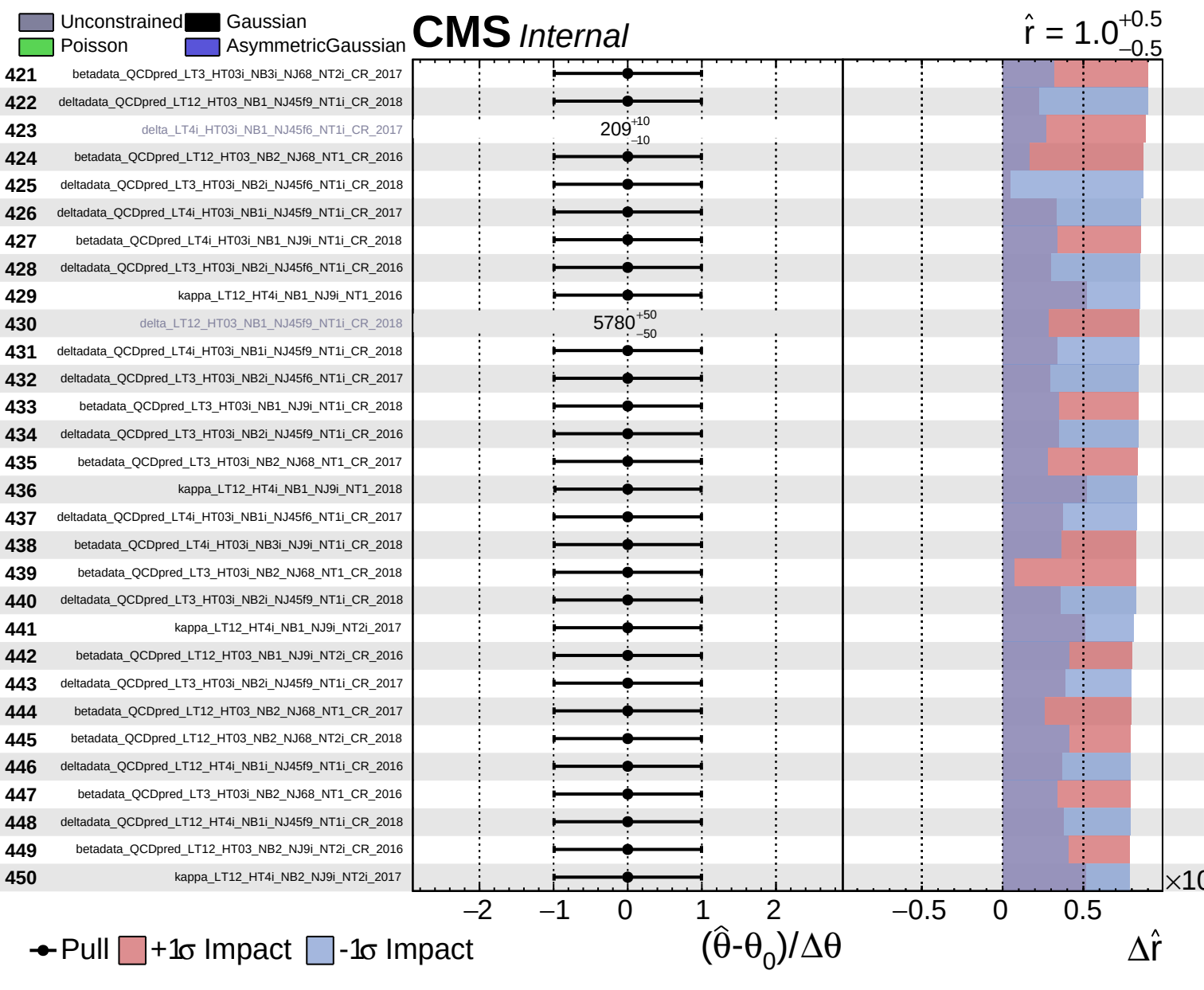
Unconstrained
Gaussian
Poisson
AsymmetricGaussian
CMS Internal
r̂ = 1.0 +0.5 −0.5
421 betadata_QCDpred_LT3_HT03i_NB3i_NJ68_NT2i_CR_2017
422 deltadata_QCDpred_LT12_HT03_NB1_NJ45f9_NT1i_CR_2018
423 delta_LT4i_HT03i_NB1_NJ45f6_NT1i_CR_2017
209 +10 −10
424 betadata_QCDpred_LT12_HT03_NB2_NJ68_NT1_CR_2016
425 deltadata_QCDpred_LT3_HT03i_NB2i_NJ45f6_NT1i_CR_2018
426 deltadata_QCDpred_LT4i_HT03i_NB1i_NJ45f9_NT1i_CR_2017
427 betadata_QCDpred_LT4i_HT03i_NB1_NJ9i_NT1i_CR_2018
428 deltadata_QCDpred_LT3_HT03i_NB2i_NJ45f6_NT1i_CR_2016
429 kappa_LT12_HT4i_NB1_NJ9i_NT1_2016
430 delta_LT12_HT03_NB1_NJ45f9_NT1i_CR_2018
5780 +50 −50
431 deltadata_QCDpred_LT4i_HT03i_NB1i_NJ45f9_NT1i_CR_2018
432 deltadata_QCDpred_LT3_HT03i_NB2i_NJ45f6_NT1i_CR_2017
433 betadata_QCDpred_LT3_HT03i_NB1_NJ9i_NT1i_CR_2018
434 deltadata_QCDpred_LT3_HT03i_NB2i_NJ45f9_NT1i_CR_2016
435 betadata_QCDpred_LT3_HT03i_NB2_NJ68_NT1_CR_2017
436 kappa_LT12_HT4i_NB1_NJ9i_NT1_2018
437 deltadata_QCDpred_LT4i_HT03i_NB1i_NJ45f6_NT1i_CR_2017
438 betadata_QCDpred_LT4i_HT03i_NB3i_NJ9i_NT1i_CR_2018
439 betadata_QCDpred_LT3_HT03i_NB2_NJ68_NT1_CR_2018
440 deltadata_QCDpred_LT3_HT03i_NB2i_NJ45f9_NT1i_CR_2018
441 kappa_LT12_HT4i_NB1_NJ9i_NT2i_2017
442 betadata_QCDpred_LT12_HT03_NB1_NJ9i_NT2i_CR_2016
443 deltadata_QCDpred_LT3_HT03i_NB2i_NJ45f9_NT1i_CR_2017
444 betadata_QCDpred_LT12_HT03_NB2_NJ68_NT1_CR_2017
445 betadata_QCDpred_LT12_HT03_NB2_NJ68_NT2i_CR_2018
446 deltadata_QCDpred_LT12_HT4i_NB1i_NJ45f9_NT1i_CR_2016
447 betadata_QCDpred_LT3_HT03i_NB2_NJ68_NT1_CR_2016
448 deltadata_QCDpred_LT12_HT4i_NB1i_NJ45f9_NT1i_CR_2018
449 betadata_QCDpred_LT12_HT03_NB2_NJ9i_NT2i_CR_2016
450 kappa_LT12_HT4i_NB2_NJ9i_NT2i_2017
×10
−2 −1 0 1 2
−0.5 0 0.5
Pull +1σ Impact -1σ Impact
(θ̂-θ0)/Δθ
Δr̂

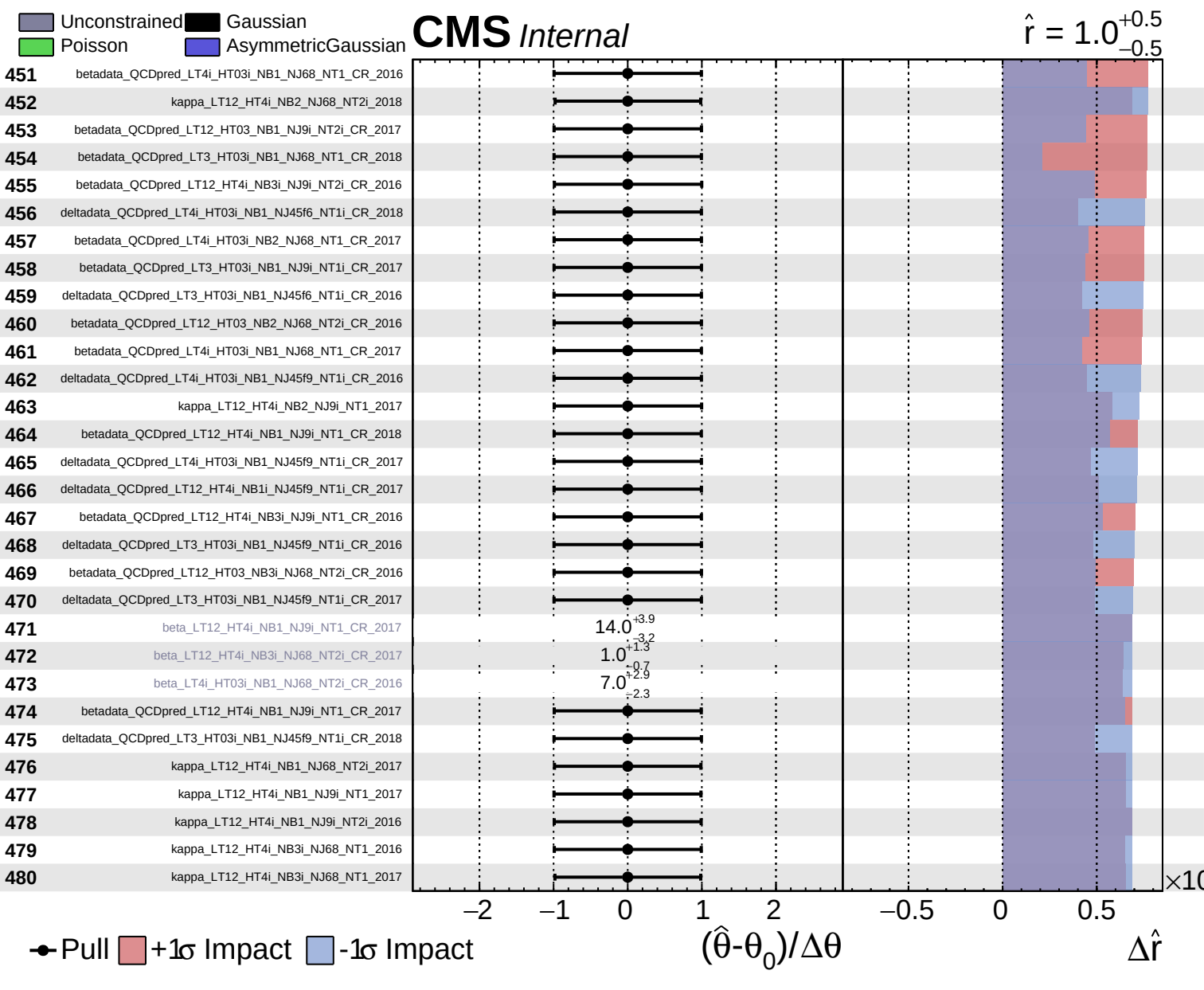
Unconstrained
Gaussian
Poisson
AsymmetricGaussian
CMS Internal
r̂ = 1.0 +0.5 −0.5
451 betadata_QCDpred_LT4i_HT03i_NB1_NJ68_NT1_CR_2016
452 kappa_LT12_HT4i_NB2_NJ68_NT2i_2018
453 betadata_QCDpred_LT12_HT03_NB1_NJ9i_NT2i_CR_2017
454 betadata_QCDpred_LT3_HT03i_NB1_NJ68_NT1_CR_2018
455 betadata_QCDpred_LT12_HT4i_NB3i_NJ9i_NT2i_CR_2016
456 deltadata_QCDpred_LT4i_HT03i_NB1_NJ45f6_NT1i_CR_2018
457 betadata_QCDpred_LT4i_HT03i_NB2_NJ68_NT1_CR_2017
458 betadata_QCDpred_LT3_HT03i_NB1_NJ9i_NT1i_CR_2017
459 deltadata_QCDpred_LT3_HT03i_NB1_NJ45f6_NT1i_CR_2016
460 betadata_QCDpred_LT12_HT03_NB2_NJ68_NT2i_CR_2016
461 betadata_QCDpred_LT4i_HT03i_NB1_NJ68_NT1_CR_2017
462 deltadata_QCDpred_LT4i_HT03i_NB1_NJ45f9_NT1i_CR_2016
463 kappa_LT12_HT4i_NB2_NJ9i_NT1_2017
464 betadata_QCDpred_LT12_HT4i_NB1_NJ9i_NT1_CR_2018
465 deltadata_QCDpred_LT4i_HT03i_NB1_NJ45f9_NT1i_CR_2017
466 deltadata_QCDpred_LT12_HT4i_NB1i_NJ45f9_NT1i_CR_2017
467 betadata_QCDpred_LT12_HT4i_NB3i_NJ9i_NT1_CR_2016
468 deltadata_QCDpred_LT3_HT03i_NB1_NJ45f9_NT1i_CR_2016
469 betadata_QCDpred_LT12_HT03_NB3i_NJ68_NT2i_CR_2016
470 deltadata_QCDpred_LT3_HT03i_NB1_NJ45f9_NT1i_CR_2017
471 beta_LT12_HT4i_NB1_NJ9i_NT1_CR_2017
472 beta_LT12_HT4i_NB3i_NJ68_NT2i_CR_2017
473 beta_LT4i_HT03i_NB1_NJ68_NT2i_CR_2016
14.0 +3.9 −3.2
1.0 +1.3 −0.7
7.0 +2.9 −2.3
474 betadata_QCDpred_LT12_HT4i_NB1_NJ9i_NT1_CR_2017
475 deltadata_QCDpred_LT3_HT03i_NB1_NJ45f9_NT1i_CR_2018
476 kappa_LT12_HT4i_NB1_NJ68_NT2i_2017
477 kappa_LT12_HT4i_NB1_NJ9i_NT1_2017
478 kappa_LT12_HT4i_NB1_NJ9i_NT2i_2016
479 kappa_LT12_HT4i_NB3i_NJ68_NT1_2016
480 kappa_LT12_HT4i_NB3i_NJ68_NT1_2017
×10
−2 −1 0 1 2
−0.5 0 0.5
Pull
+1σ Impact
-1σ Impact
(θ̂-θ0)/Δθ
Δr̂

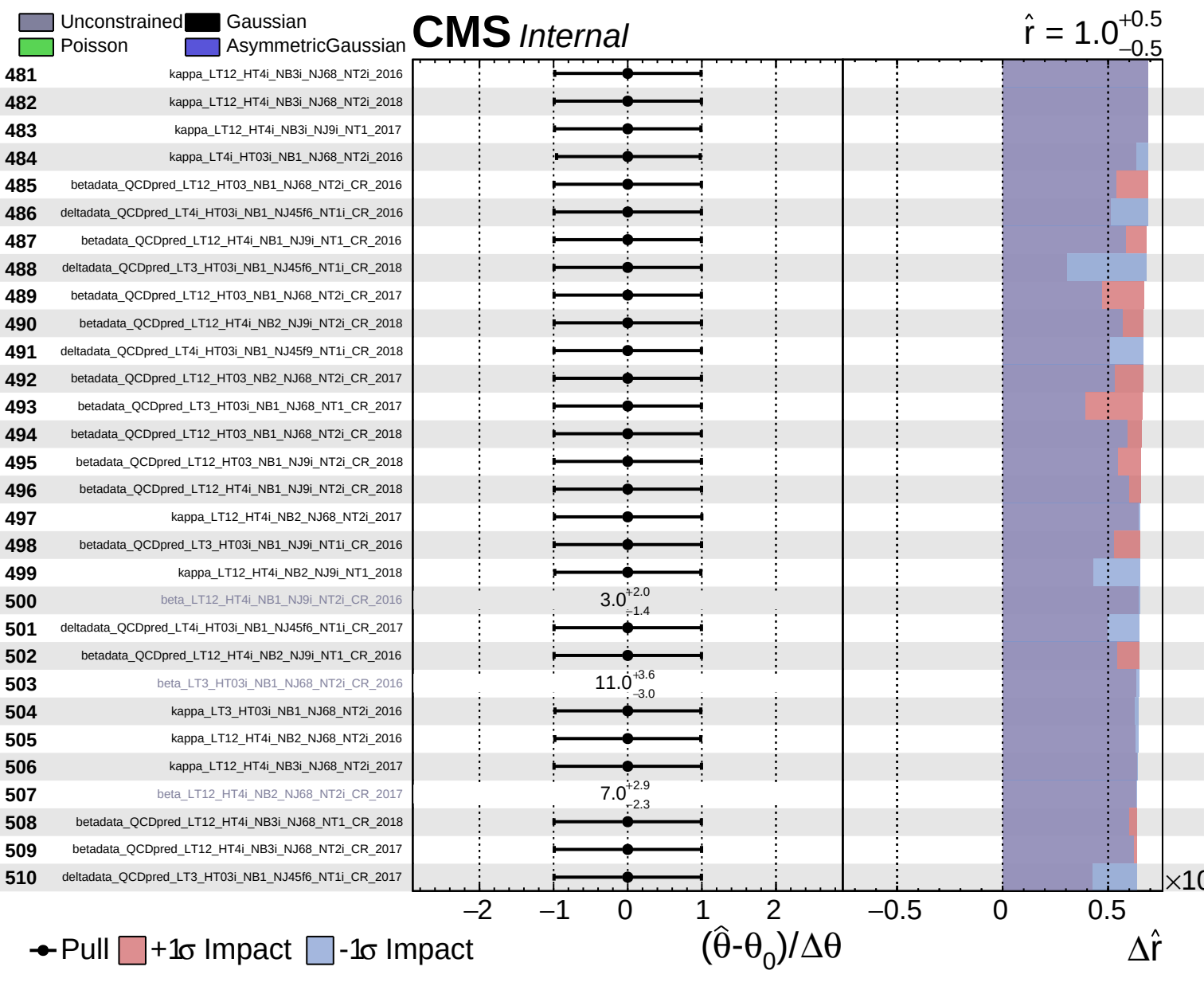
Unconstrained
Gaussian
Poisson
AsymmetricGaussian
CMS Internal
$\hat{r} = 1.0^{+0.5}_{-0.5}$
481 kappa_LT12_HT4i_NB3i_NJ68_NT2i_2016
482 kappa_LT12_HT4i_NB3i_NJ68_NT2i_2018
483 kappa_LT12_HT4i_NB3i_NJ9i_NT1_2017
484 kappa_LT4i_HT03i_NB1_NJ68_NT2i_2016
485 betadata_QCDpred_LT12_HT03_NB1_NJ68_NT2i_CR_2016
486 deltadata_QCDpred_LT4i_HT03i_NB1_NJ45f6_NT1i_CR_2016
487 betadata_QCDpred_LT12_HT4i_NB1_NJ9i_NT1_CR_2016
488 deltadata_QCDpred_LT3_HT03i_NB1_NJ45f6_NT1i_CR_2018
489 betadata_QCDpred_LT12_HT03_NB1_NJ68_NT2i_CR_2017
490 betadata_QCDpred_LT12_HT4i_NB2_NJ9i_NT2i_CR_2018
491 deltadata_QCDpred_LT4i_HT03i_NB1_NJ45f9_NT1i_CR_2018
492 betadata_QCDpred_LT12_HT03_NB2_NJ68_NT2i_CR_2017
493 betadata_QCDpred_LT3_HT03i_NB1_NJ68_NT1_CR_2017
494 betadata_QCDpred_LT12_HT03_NB1_NJ68_NT2i_CR_2018
495 betadata_QCDpred_LT12_HT03_NB1_NJ9i_NT2i_CR_2018
496 betadata_QCDpred_LT12_HT4i_NB1_NJ9i_NT2i_CR_2018
497 kappa_LT12_HT4i_NB2_NJ68_NT2i_2017
498 betadata_QCDpred_LT3_HT03i_NB1_NJ9i_NT1i_CR_2016
499 kappa_LT12_HT4i_NB2_NJ9i_NT1_2018
500 beta_LT12_HT4i_NB1_NJ9i_NT2i_CR_2016
$3.0^{+2.0}_{-1.4}$
501 deltadata_QCDpred_LT4i_HT03i_NB1_NJ45f6_NT1i_CR_2017
502 betadata_QCDpred_LT12_HT4i_NB2_NJ9i_NT1_CR_2016
503 beta_LT3_HT03i_NB1_NJ68_NT2i_CR_2016
$11.0^{+3.6}_{-3.0}$
504 kappa_LT3_HT03i_NB1_NJ68_NT2i_2016
505 kappa_LT12_HT4i_NB2_NJ68_NT2i_2016
506 kappa_LT12_HT4i_NB3i_NJ68_NT2i_2017
507 beta_LT12_HT4i_NB2_NJ68_NT2i_CR_2017
$7.0^{+2.9}_{-2.3}$
508 betadata_QCDpred_LT12_HT4i_NB3i_NJ68_NT1_CR_2018
509 betadata_QCDpred_LT12_HT4i_NB3i_NJ68_NT2i_CR_2017
510 deltadata_QCDpred_LT3_HT03i_NB1_NJ45f6_NT1i_CR_2017
×10
−2 −1 0 1 2
−0.5 0 0.5
Pull
+1σ Impact
-1σ Impact
$(\hat{\theta}-\theta_0)/\Delta\theta$
$\Delta\hat{r}$

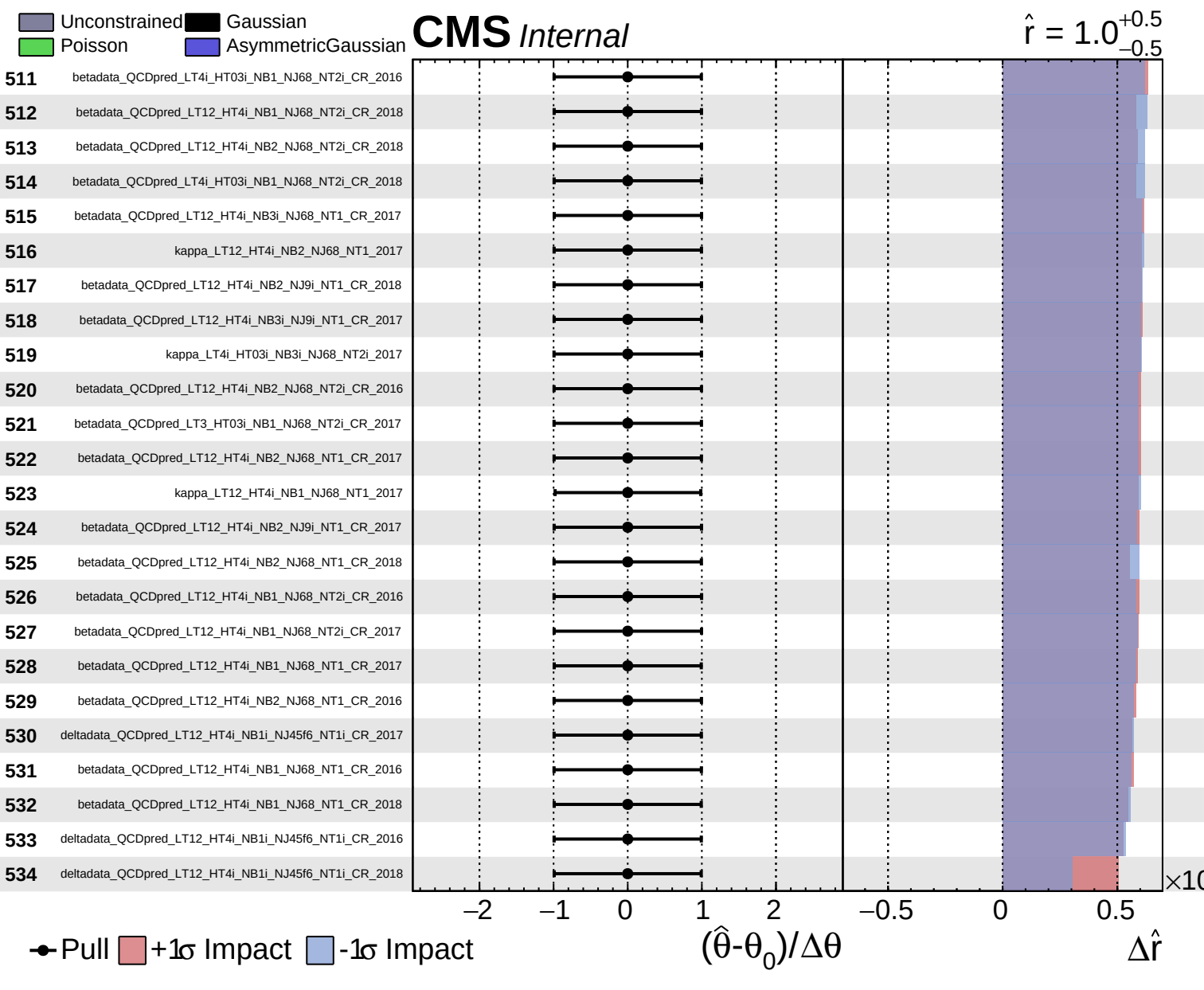
Unconstrained
Gaussian
Poisson
AsymmetricGaussian
CMS Internal
r̂ = 1.0 +0.5 −0.5
511 betadata_QCDpred_LT4i_HT03i_NB1_NJ68_NT2i_CR_2016
512 betadata_QCDpred_LT12_HT4i_NB1_NJ68_NT2i_CR_2018
513 betadata_QCDpred_LT12_HT4i_NB2_NJ68_NT2i_CR_2018
514 betadata_QCDpred_LT4i_HT03i_NB1_NJ68_NT2i_CR_2018
515 betadata_QCDpred_LT12_HT4i_NB3i_NJ68_NT1_CR_2017
516 kappa_LT12_HT4i_NB2_NJ68_NT1_2017
517 betadata_QCDpred_LT12_HT4i_NB2_NJ9i_NT1_CR_2018
518 betadata_QCDpred_LT12_HT4i_NB3i_NJ9i_NT1_CR_2017
519 kappa_LT4i_HT03i_NB3i_NJ68_NT2i_2017
520 betadata_QCDpred_LT12_HT4i_NB2_NJ68_NT2i_CR_2016
521 betadata_QCDpred_LT3_HT03i_NB1_NJ68_NT2i_CR_2017
522 betadata_QCDpred_LT12_HT4i_NB2_NJ68_NT1_CR_2017
523 kappa_LT12_HT4i_NB1_NJ68_NT1_2017
524 betadata_QCDpred_LT12_HT4i_NB2_NJ9i_NT1_CR_2017
525 betadata_QCDpred_LT12_HT4i_NB2_NJ68_NT1_CR_2018
526 betadata_QCDpred_LT12_HT4i_NB1_NJ68_NT2i_CR_2016
527 betadata_QCDpred_LT12_HT4i_NB1_NJ68_NT2i_CR_2017
528 betadata_QCDpred_LT12_HT4i_NB1_NJ68_NT1_CR_2017
529 betadata_QCDpred_LT12_HT4i_NB2_NJ68_NT1_CR_2016
530 deltadata_QCDpred_LT12_HT4i_NB1i_NJ45f6_NT1i_CR_2017
531 betadata_QCDpred_LT12_HT4i_NB1_NJ68_NT1_CR_2016
532 betadata_QCDpred_LT12_HT4i_NB1_NJ68_NT1_CR_2018
533 deltadata_QCDpred_LT12_HT4i_NB1i_NJ45f6_NT1i_CR_2016
534 deltadata_QCDpred_LT12_HT4i_NB1i_NJ45f6_NT1i_CR_2018
−2 −1 0 1 2
−0.5 0 0.5
×10
Pull +1σ Impact -1σ Impact
(θ̂-θ0)/Δθ
Δr̂